Development of an Integrated Transport and Emissions Model and Applications for Population Exposure and Environmental Justice

Timothy Sider

Thesis

Department of Civil Engineering and Applied Mechanics
McGill University, Montréal

December 2013

Thesis submitted to McGill University in partial fulfillment
of the requirements for the degree of Master of Engineering

CONTRIBUTION OF AUTHORS

A number of other researchers have contributed to the work found in this thesis. The two major contributors are my co-supervisors, Professors Marianne Hatzopoulou and Naveen Eluru, who co-authored the three research papers found in Chapters 4-6. For development of the integrated transport and emission model, assistance was received from: William Farrell (M.Eng candidate) for the regional assignment model; Ahsan Alam (PhD candidate) for the running emission simulation; and Gabriel Goulet-Langlois (B.Eng candidate) for the running and start emission simulations. Gabriel Goulet-Langlois also contributed work to the research on variability of emission estimates in Chapter 4. Meanwhile, Chapter 5 was co-authored by Ahsan Alam, Mohamad Zukari (B.Eng candidate), Hussam Dugum (B.Eng candidate), and Nathan Goldstein (B.Eng candidate). Finally, Chapter 6 was written in collaboration with Professor Kevin Manaugh.

ACKNOWLEDGEMENTS

I would first like to acknowledge my two co-supervisors, Professors Marianne Hatzopoulou and Naveen Eluru, for their tremendous support and guidance over the past two and a half years. It has been a great privilege to have both as supervisors. I would also like to thank other graduate students in the transportation program that I've collaborated with, specifically William Farrell and Ahsan Alam. At the same time, contribution to the research from a number of undergraduate students has been invaluable. This includes Gabriel Goulet-Langlois, Mohamad Zukari, Hussam Dugum, Nathan Goldstein, and Anthony Somos. Furthermore, I would like to acknowledge the teachings of Professors Peter Brown, Mark Goldberg and Nicolas Kosoy for inspiring the philosophical basis for my research into the environmental and social impacts of our transportation systems. Finally, I would like to thank my parents, my brother and my girlfriend, for being awesome. Much love.

ABSTRACT

Road transport has a tremendous impact on local urban regions as well as global planetary health. This impact is especially great given the large quantities of greenhouse gases and local air pollutants released across the world, quantities that continue to increase. For metropolitan regions, reductions in traffic-related air pollution are paramount. Which baseline is used and which strategies should be implemented are both vital questions in this regard. Integrated transport and emissions models are important tools that aid metropolitan planners in answering those questions. A regional traffic assignment model has been connected to a detailed emission processor for the Montreal metropolitan region. The road transport model contains details on all private driving trips across a standard 24-hr workday, including congested link speeds and stochastic path distributions. Meanwhile, the emissions processor incorporates local vehicle registry data and Montreal-specific ambient conditions in the estimation of both running and start emissions. Outputs include hourly link-level and trip-level emissions for greenhouse gases, hydrocarbons, and nitrogen oxides. Three research studies were then explored that were anchored by the integrated transport and emissions model. The first involved testing model sensitivity to variations in input data and randomness. The second study was aimed at understanding the land-use and socioeconomic determinants of traffic-related air pollution generation and exposure. The third study encompassed an equity analysis of social disadvantage, traffic-related air pollution generation and exposure. Major findings include evidence that: start emissions and accurate vehicle registry data have the biggest impact on accurate regional emission inventories; neighbourhoods closer to downtown tend to be low emitters while having high exposures to traffic-related air pollution, while the opposite is true for neighbourhoods in the suburbs and periphery of the region; and marginalized neighbourhoods with high social disadvantage tend to have the highest exposure levels in the region, while at the same time generating some of the lowest quantities of traffic-related air pollution. These findings support the claim that traffic is creating environmental justice issues at the metropolitan level.

RÉSUMÉ

L'impact des systèmes de transports sur les régions urbaines et la santé planétaire est immense. Cet impact est notamment important parce-que les quantités de gaz à effet de serre et les polluants atmosphériques continuent à augmenter autour du monde. Pour les régions métropolitaines, les réductions de la pollution de l'air liée à la circulation sont essentielles. Cependant, quel point de référence est appliqué, et quelles stratégies devraient être mises en œuvre, sont deux questions vitales à cet égard. Une simulation intégrée du transport et des émissions est un outil important qui aide les planificateurs à répondre à ces questions. Une simulation de la circulation régionale a été liée à un simulateur des émissions détaillées pour la région métropolitaine de Montréal. La simulation de la circulation contient des détails sur tous les déplacements 'auto conducteur' pour chaque heure d'une journée normale de travail, incluant la vitesse de circulation encombrée, et distributions des trajets stochastiques. Aussi, le simulateur des émissions incorpore des données sur les types de véhicules et les conditions ambiantes locales dans l'estimation des émissions de conduite et d'ignition. Les données produisent sont des quantités d'émissions horaires au niveau des routes et des déplacements pour les gaz a effet de serre, les hydrocarbures, et les oxydes d'azote. Trois études de recherche ont été basées sur les résultats de la simulation intégrée de la circulation et des émissions. La première examine la sensibilité de la simulation aux variations dans les données. La deuxième évalue si l'utilisation du sol ou les caractéristiques socio-économiques sont les déterminants de production ou d'exposition à la pollution de l'air liée à la circulation. La troisième inclue une analyse du désavantage social et de la production et de l'exposition à la pollution de l'air liée à la circulation. On observe que les émissions à l'ignition et les données d'immatriculation des véhicules ont le plus grand impact sur les inventaires des émissions régionales. En terme d'exposition à la pollution de l'air, les quartiers les plus proches du centre-ville ont tendance à produire le moins d'émissions tandis qu'ils ont les niveaux d'exposition les plus élevés dans la région, alors que l'inverse est vrai pour les quartiers de banlieue et à la périphérie. Les quartiers caractérisés par un index de désavantage social élevé ont les niveaux

d’exposition les plus élevés et en même temps produisent de faibles taux d’émissions. Ces résultats appuient l’hypothèse que la circulation contribue aux problèmes de justice environnementale à l’échelle métropolitaine.

TABLE OF CONTENTS

LIST OF TABLES

LIST OF FIGURES

LIST OF ABBREVIATIONS

AMT – Agence Métropolitaine de Transport

CBD – Central Business District

CO – Carbon Monoxide

CO_2 – Carbon Dioxide

CT – Census Tract

EF – Emission Factor

FSA – Forward Sorting Area

HC – Hydrocarbons

MMR – Montreal Metropolitan Region

MOVES – Mobile Vehicle Emissions Simulator

NO_2 – Nitrogen Dioxide

NO_x – Nitrogen Oxides

OD – Origin-Destination

PC – Passenger Car

PM – Particulate Matter

PPP – Polluter-Pays Principle

PT – Passenger Truck

SAAQ – Société de l'Assurance Automobile du Québec

SDI – Social Disadvantage Index

SE – Standard Error

SUV – Suburban Utility Vehicle

TAZ – Traffic Analysis Zone

TOD – Transit Oriented Development

USEPA – United States Environmental Protection Agency

VKT – Vehicle-Kilometres-Travelled

VOC – Volatile Organic Compound

CHAPTER 1:
INTRODUCTION

1.1 Background

Transportation and its negative externalities have a significant impact on global planetary health. As a sector, transport contributes 13.1 percent of global greenhouse gas (GHG) emissions (IPCC, 2007) and 24 percent of Canada's GHG footprint (Environment Canada, 2011). Additionally, nearly half the world's oil usage is attributed to motorized transport, further increasing its total contribution (Woodcock et al., 2007). Furthermore, on-road emissions are predicted to have the highest impact on climate forcing of any economic sector in the near future (10-15 years), and the second highest impact over the long-term (100 years; Unger et al., 2010). Road-transport, consisting of private light-duty cars and trucks, public transit vehicles and heavy-duty freight trucks, is specifically estimated to make up almost three-quarters of transport's total contribution (IEA, 2012). While technological improvements have lowered emission rates per vehicle, increases in total vehicle-kilometres-travelled (VKT) have negated most of those gains.

At the same time, the negative externalities from road-transport have a significant presence in urban environments. With the disappearance of urban industry over the last few decades, road transport has now become the largest contributor of air pollution in urban regions (Colvile et al., 2001). Local air pollutants from road transport come in the form of carbon monoxide (CO), hydrocarbons (HC), nitrogen oxides (NO_x), and particulate matter (PM), while also contributing significant amounts of noise pollution. Previous studies have found considerable evidence that long-term exposure to local traffic-related air and noise pollution is potentially dangerous to various aspects of human health including birth outcomes (Brauer et al., 2008), children's health (Kim et al., 2004; Zmirou et al., 2004; Kramer et al., 2000) and respiratory and cardiovascular diseases, including lung cancer (Gan et al., 2012; Selander et al., 2009; Chen et al., 2008; Babisch et al., 2005; Hoek et al., 2002; and Kunzli et al., 2000).

Given the challenges that metropolitan regions face, road transport's impact must be reduced. Planners and policymakers need tools in this regard that aid in quantifying the problem and assessing feasible solutions. Integrated transport and emission models are the best bet in this respect. Integrated models combine two streams of research through linkages between transportation modeling and detailed emission modeling, a combined focus that has grown rapidly in the past few years in light of the aforementioned issues facing metropolitan regions and the global community at large. These integrated transport and emission models are a crucial element for metropolitan planners in answering questions such as: What is the carbon footprint of our metropolitan region? Who are the highest emitters? Which neighbourhoods experience the greatest levels of traffic-related air pollution? What steps need to be taken to reduce emissions by 15, 20, or 25%? The purpose of this thesis is therefore to explore the various applications of an integrated transport and emissions model with a focus on the Montreal region.

1.2 Objectives

The objectives of this thesis are as follows:

i. Development of a regional traffic assignment model for the Montreal metropolitan region (MMR)
ii. Creation of an integrated transport and emission model that incorporates the following details in an emission processor:
    a. Vehicle allocation
    b. Running emissions
    c. Start emissions
iii. Evaluation of the sensitivity of emission estimates from integrated transport and emission models to data inputs and model randomness
iv. Assessment of the extent that land-use and socioeconomic characteristics play in determining traffic-related air pollution generation and exposure at the zonal level in the MMR
v. Exploration of the equity of traffic-related air pollution generation, exposure and socioeconomic status across the MMR

1.3 Thesis structure

The thesis begins with an overview of the context of this research. Specifically, previous research into integrated transport and emission models is explored and a summary of the study area (MMR) is included. From there, an entire section is devoted to model development, which explores the creation of the regional traffic assignment model, the emission processor, and validation of both models. The following three chapters cover three individual research papers that were anchored by the integrated transport and emissions model:

- Chapter 4: Sensitivity of emission estimates
- Chapter 5: Determinants of emissions generation and exposure
- Chapter 6: Equity analysis

Each chapter has context-specific sections on literature review, methodology, results and discussion. Finally, the thesis concludes with a summary of major findings as well as a short overview regarding pathways of future research.

CHAPTER 2:
CONTEXT

2.1 Integrated transportation and emission models

Research into accurately estimating emissions from road transport has been growing over the past few decades. Unlike the estimation processes for stationary sources such as power plants, estimating exhaust levels from mobile sources such as road transport is quite difficult due to the numerous dimensions involved, such as travel speeds, vehicle characteristics, ambient conditions, and more. Focussing on private individual travel, instead of public or freight, has still resulted in a large variety in emission models. To begin, it is important to define the term 'emission model' and to describe how it interacts with transportation data inputs.

Emission modeling of mobile sources involves the use of a modeling platform to simulate all types of emissions resulting from motor vehicles. Specifically, this includes those occurring at engine ignition (start emissions), during vehicle cruising (running emissions) and after engine shutdown (evaporative or soak emissions). Running emissions have been the focus of most research given that they typically constitute the majority of pollution emitted (Borrego et al., 2004; Houk, 2004). A modeling platform is therefore used to generate running emission factors (EFs) that dictate a relationship between vehicle, speed and quantity of emitted pollutant. For instance, if a vehicle with specific characteristics (type, model year, engine size, fuel type, presence of catalytic converter, etc.) drives at a given speed with a certain behaviour (acceleration, deceleration, gradient) and under particular ambient conditions (temperature, pressure, sun-exposure, etc.), then it has an associated EF in grams per VKT. Transportation data comes into the equation through travel speed and VKT, both considered crucial elements in emission estimation (Smit, 2006). Overall, emission models from the previous two decades span a wide spectrum of complexity, however this trend is neither time dependent nor geographical in nature (ie. concentrated in developed, Western nations). Emission models have certainly become more complex in general, yet

varying research objectives or data availability continue to favour the use of simple models in many situations.

The simplest models are typically used to estimate basic national emission inventories, for instance in Mexico (Solis and Sheinbaum, 2013), or in research that studies the determinants of individual/household GHG footprints in regions such as Quebec City, Canada (Barla et al., 2011), Seoul, South Korea (Ko et al., 2011), and Oxford, England (Brand and Preston, 2010). Numerous assumptions must be made across many of the model inputs. Transportation data is sourced from stated VKT estimates from travel surveys, and then EFs derived from average local fuel consumption rates are applied assuming a constant average vehicle speed. Another set of models combine similar travel survey data with EFs generated from an emission simulator. In North America, specifically in the Puget Sound region of Washington (Frank et al., 2006; Frank et al., 2000), the MOBILE series of emission modeling software developed by the United States Environmental Protection Agency (USEPA) was used to generate more accurate EFs for a range of pollutants and vehicle characteristics. A comparable approach was also taken in Europe, specifically in the Sardinia region in Italy (Bellasio et al., 2007), using the COPERT platform developed by the European Environmental Agency (EEA). Lumbreras et al (2013) even developed a platform that created more accurate transport and vehicle data for use in the COPERT emission simulator in order to estimate emissions for the entire country of Spain. While these types of models attempt to account for congestion in their composite EFs, assumptions are still made regarding vehicle characteristics, and no sense of spatial or temporal variation across their study areas is possible.

The spatial distribution of traffic-related air pollution on the road network is paramount for the analysis of NO_x, HCs, PM, and other local pollutants, especially given that intra-urban variation can be larger than inter-urban variation (Crouse et al., 2009a). Another set of models attempts to incorporate spatial issues through the use of manual traffic counts as the transport data input. This process also

usually captures local variations in vehicle composition, and has been applied to the northwest of England (Lindley et al., 1999), Beijing, China (Hao et al., 2000), Santiago, Chile (Corvalan et al., 2002), and Beirut, Lebanon (Waked and Afif, 2012). Corvalan et al (2002) are even able to account for temporal variation by using hourly counts.

However, the majority of research has focussed on the development of truly integrated transport and emission models incorporating detailed road-traffic simulations. Road-traffic networks are modeled at a macroscopic or mesoscopic scale, and then trips are assigned to the network on an hourly basis. Output data include VKT and average link speeds, which are both used directly in conjunction with the EFs generated from the emissions simulator. This process has garnered international popularity and has been employed in cities and regions such as Hamilton, Canada (Anderson et al., 1996), Helsinki, Finland (Karppinen et al., 2000), Antwerp, Belgium (Mensink et al., 2000), Lisbon, Portugal (Borrego et al., 2004), Hong Kong, China (Xia and Shao, 2005), Norwich, England (Nejadkoorki et al., 2008), and Madrid, Spain (Borge et al., 2012). Beckx et al (2009a) and Hao et al (2010) even incorporated activity-based models into their integrated modeling frameworks applied respectively to the Netherlands and the Greater Toronto Area, Canada. The advantage of integrated transport and emission models is that they are able to combine congestion-related speed effects and detailed vehicle data, often at the individual trip level. This provides significant detail regarding spatial and temporal variation, and allows for connections to socioeconomics or even to dispersion models that portray how meteorological conditions and the built environment influence pollutant concentrations (De Ridder et al., 2008).

Meanwhile, start emissions occur at engine ignition and typically occur during the first two to three minutes of a trip. They are considered separate from those that are emitted during an engine's cruising phase, and they are mostly caused by: (1) excess gasoline due to higher fuel enrichment; and (2) poor catalytic converter

performance due to the large gap between engine temperature at ignition and optimum temperature for catalytic conversion. The gap between engine and optimum temperatures is dependent on the ambient temperature, which varies by season, and the engine's ignition temperature, which is related to the engine soak-time, ie. the amount of time since the engine was turned off. Therefore, an engine that had been turned off recently would have a smaller soak-time and thus would have an ignition temperature that is closer to the optimum temperature of the catalytic converter. Start emissions are especially of concern when studying HC, CO or NO_x emissions, accounting for approximately 28 percent, 31 percent and 20 percent of total on-road VOCs, CO and NO_x, respectively (Houk, 2004). Previous research that had employed the MOBILE platform implicitly account for start emissions through the generated running EFs (Hao et al., 2010; Frank et al., 2006; Frank et al., 2000; Anderson et al., 1996). COPERT models account for starts in a similar fashion (Lumbreras et al., 2013; Waked and Afif, 2013; Bellasio et al., 2007). The current generation of emission software favours a distinct separation between running and start emissions, with start EFs used to dictate the relationship between vehicle characteristics, soak-time and amount of pollutants emitted during engine ignition.

This research aims to build on the advancements in integrated transport and emission models through the development of a connected regional traffic assignment model and a comprehensive emission processor. The regional traffic assignment model provides accurate average link speed and VKT data, while accurate vehicle registry data is also incorporated. An emission simulator is used to generate both running and start EFs.

2.2 Study Area

Our study area includes the MMR, which covers an area of approximately 7,000 km^2 and has a population of about 3.8 million (Statistics Canada, 2011). The region is dominated by the island of Montreal, with approximately 47 percent of the region's population and 71 percent of the region's 1.4 million employment

opportunities (AMT, 2010). The remainder of the region consists of two sub-regions north of Montreal: Laval and the twenty municipalities of the North Shore, and another two sub-regions south of the island: Longueuil and the twenty-five South Shore municipalities. Figure 1 provides the population distribution in terms of density across the MMR with all the major sub-regions identified. Further, the figure identifies the central business district (CBD) in a red box.

Figure 1 – Population density of the MMR

Figure 2 highlights the major boroughs on the island of Montreal as well as the cities of Laval to the northwest and Longueuil to the east. The CBD is located within the Ville-Marie borough.

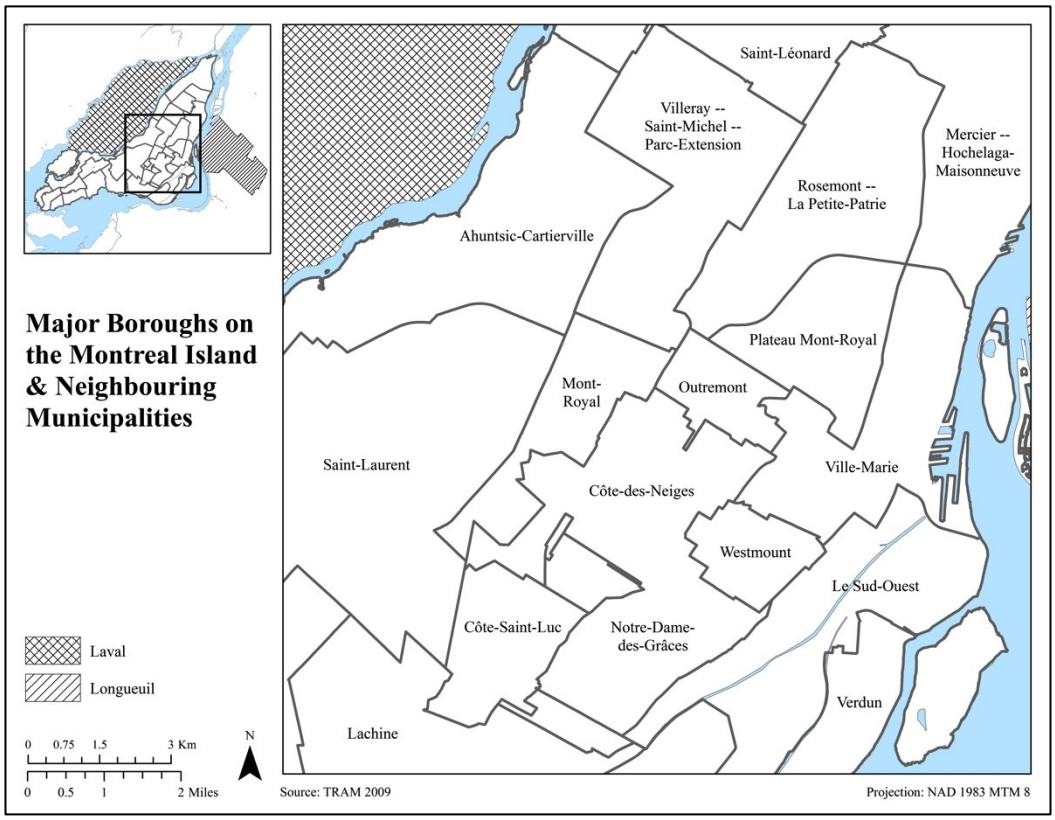

Figure 2 – Map of the Island of Montreal and surrounding municipalities

The spatial economy of the Montreal region is anchored by the CBD; 59 percent of the region's employment opportunities are within 10 km of downtown, while the remaining job distribution follows a concentric distance-decay curve (Shearmur and Coffey, 2002). The other major employment centre in the region is found near Montreal's main airport in Ville-Saint-Laurent/Dorval, located 10-15 km west of downtown. The imbalance between jobs and residents previously mentioned for the island of Montreal is especially large for the CBD and surrounding central areas. In the central areas there are 24 workers for every 10 residents, an employment surplus that is being fed by Laval, Longueuil, and other municipalities on the North and South shores (Shearmur and Motte, 2009). Meanwhile, the island of Montreal is connected to the other sub-regions through a system of bridges. Five bridges connect the island to the north and five to the south, while two bridges at either end of the island connect the peripheral eastern and western edges. With the very high proportion of off-island and on-island

commuters, bridges linking the island to the rest of the region have become the salient element of the road network. At the same time, most of the residential growth is occurring in the periphery zones of the region particularly in the north and south shore municipalities (AMT, 2010). Overall, there are over two million vehicles registered in the region, resulting in a regional household vehicle ownership rate of about 1.2 vehicles (AMT, 2010).

CHAPTER 3:
OVERALL MODEL STRUCTURE

The integrated transport and emission model has two base data inputs (OD survey, vehicle registry) and two inputs generated from commercial software (emission factors, traffic data). The primary outputs include emissions at both the link- and trip-level. Developed as part of this thesis, the emission processor is the key element of the integrated model, incorporating all four data inputs in generating the desired output (Figure 3). The emission processor consists of: (1) a vehicle allocation algorithm, (2) a running emissions model, and (3) a start emissions model. The interactions between all the elements in the integrated framework are highlighted in detail in Figure 4. The base data sources, specifically the travel behaviour information and the vehicle registry data, are described first. The platform used to generate running and start EFs is the Mobile Vehicle Emissions Simulator (MOVES) developed by the USEPA.

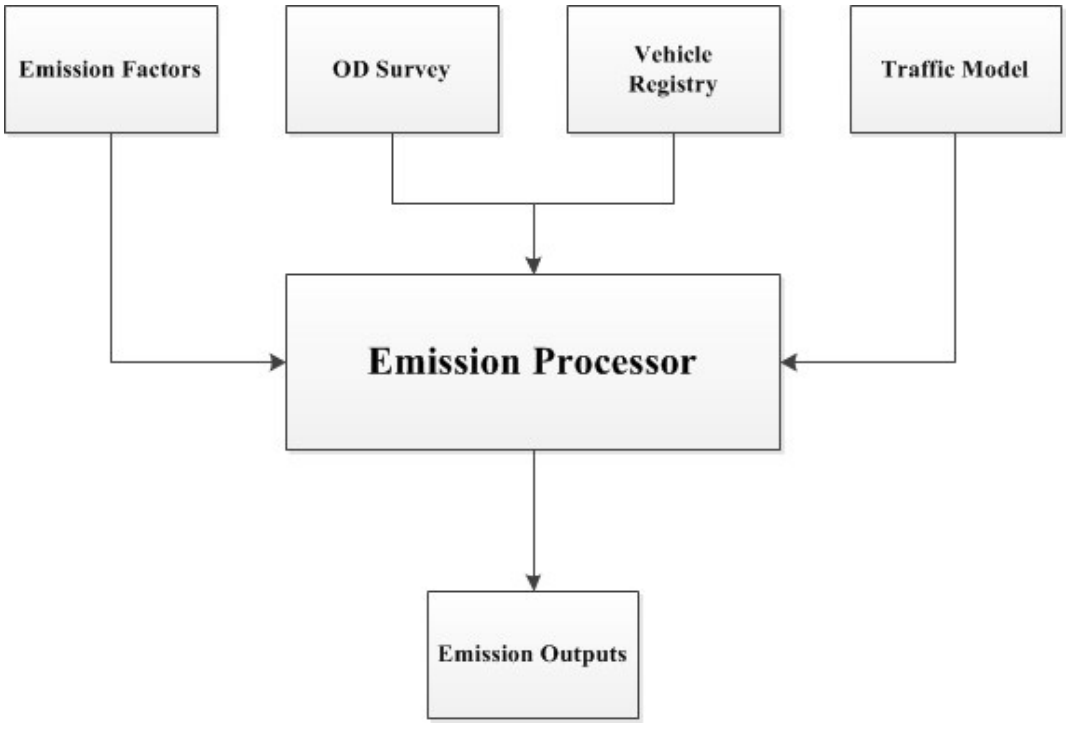

Figure 3 – Integrated modeling framework

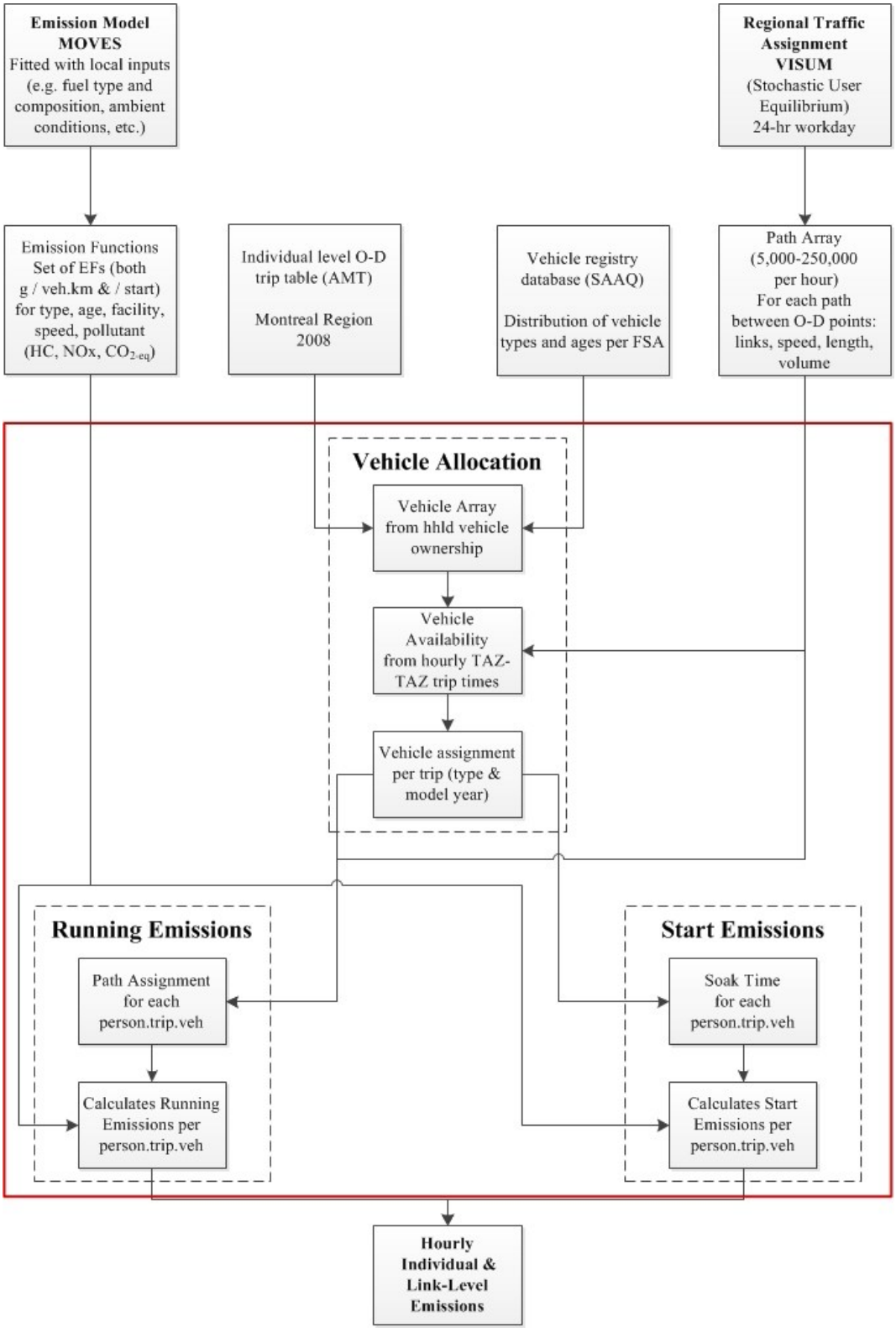

Figure 4 – Detailed framework (emission processor outlined in red)

3.1 Base Data Sources

Origin-Destination Survey

The base travel data for the integrated model encompasses the 2008 origin-destination (OD) survey conducted by the Agence Métropolitaine de Transport (AMT), the regional transit authority in the MMR. The OD survey data contains information on 319,915 trips conducted in the MMR; each trip is associated with a set of attributes including origin, destination, departure time, travel mode, and attributes of the individual performing the trip including residential location. In addition, every trip is associated with a weight or "expansion factor" which allows us to scale the sample up to the total population. This survey is conducted every five years and is the primary source in Montreal for information on travel habits. The most recent survey was conducted in 2008 and the results were released in 2010. Participants in the survey were identified through a random sample of the Montreal population using telephone listings; the sample is validated against census data using a wide range of variables (age, gender, employment status, home location, work location, etc.). In 2008, 66,100 households (representing 4% of the population) were interviewed including 156,700 individuals. Telephone interviews took place in autumn, a time period when most urban travel habits are stable.

Vehicle Registry Data

The vehicle registry database was obtained from the provincial registry at the Société de l'Assurance Automobile du Québec (SAAQ) for the base year of 2011. The SAAQ database includes vehicle ownership information for the Montreal region at the level of the Forward Sorting Area (FSA), indicated by the first three characters of the postal code. Within each FSA, the total number of vehicles by type (e.g. passenger car (PC), sports utility vehicle, minivan, small truck, large truck) and model year (1981-2011) is provided. The SAAQ data contains 12 vehicle designations. These designations were collapsed into two groups, one for PCs and one for passenger trucks (PTs; which includes SUVs, minivans, and pick-up trucks).

While it is possible that the 12 vehicle designations have different emission profiles, it is important to recognize that vehicle emissions on roadways are not only dependent on vehicle types and models but also influenced by fuel and engine technology, engine displacement, model year group, and regulatory class (USEPA, 2010). In fact the emission differences between different PCs of the same model year (and regulatory class) undergoing the same drive-cycle are smaller than emission differences for the same car undergoing different driving patterns. In real-road conditions, the differences due to vehicle make within the same category (PT or PC) can be neglected. For this reason the USEPA's model MOVES 2010 has aggregated passenger vehicles into two broad categories: (1) PCs (i.e. all sedans, coupes, and station wagons manufactured primarily for the purpose of carrying passengers) and (2) PTs (which includes SUVs, minivans, and pick-up trucks) coming from a larger vehicle classification which was included in the older MOBILE6 series. The distribution of the fleet was computed for each FSA, based on the two vehicle types and thirty model years provided.

3.2 Traffic Assignment

A regional traffic assignment model was developed for the MMR (Figure 5). The model takes as input the 2008 OD trip data for the MMR provided by the AMT and assigns it on the road network using a stochastic assignment in the VISUM platform (PTV Vision, 2009). The regional network consists of 127,217 road links and 90,467 nodes associated with 1,552 traffic analysis zones (TAZs). All levels of road types were included in the model, ranging from expressways to arterials to local roads. It also contains various road characteristics such as length, speed limit, capacity, and number of lanes, as well as intersection characteristics such as capacity and turning restrictions.

Only the driving trips were extracted from the OD survey for the purpose of this study and segmented into twenty-four 1-hour OD matrices based on trip departure times. The OD matrices were generated at the TAZ level. The simulated traffic was assigned to the network employing the stochastic user equilibrium approach

(SUE) in VISUM. The SUE approach allows for route choice distribution based on perceived travel times thus incorporating realistic route choice behavior compared to the traditional deterministic user equilibrium approach (PTV Vision, 2009). Output from the traffic assignment simulations consisted of an array that contained a detailed description of all paths connecting pairs of OD zones in all 24 hourly periods. This "path array" contains anywhere from 5,000 to 250,000 paths per hour for which the following characteristics are listed: links along the path, traffic volumes per link, average speed per link, link type and traffic volume per path.

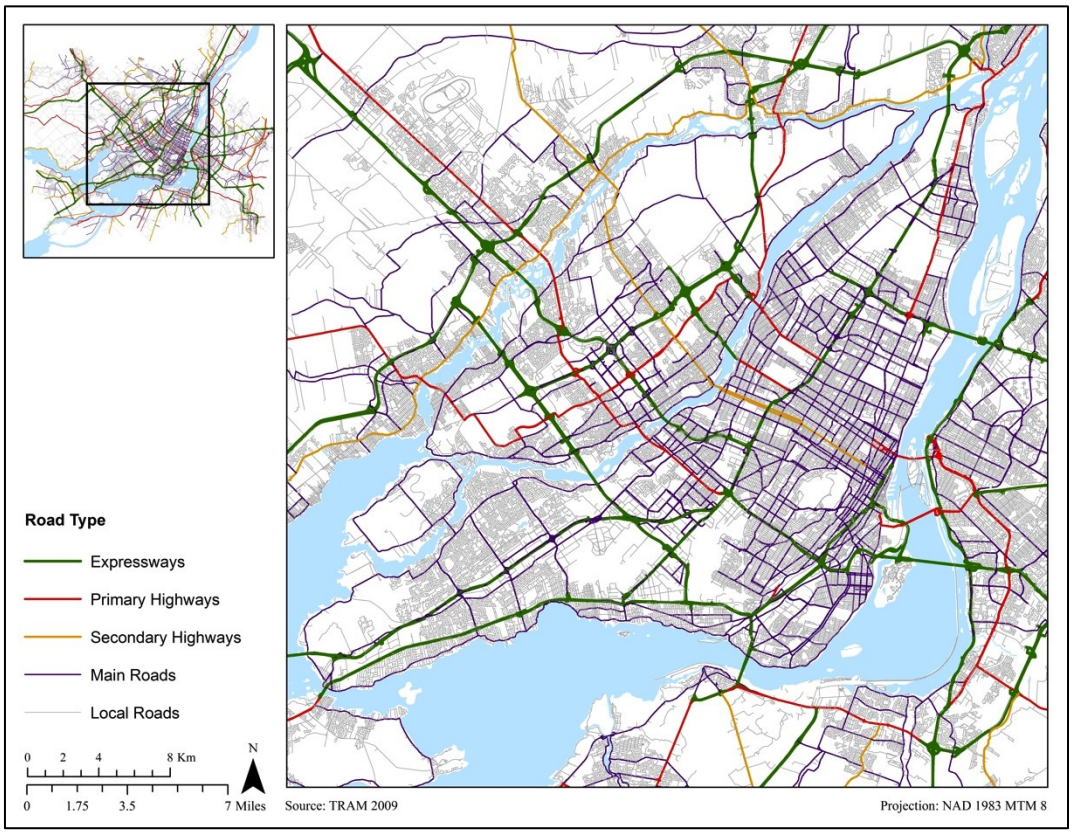

Figure 5 – Road network of the MMR

3.3 Vehicle Allocation

In order to maintain vehicle consistency between the estimation methods for running and start emissions, the first step in emission estimation involved allocating a vehicle to each of the driving trips in the 2008 OD survey (162,364

trips). Working at the household level, the main elements involved with vehicle allocation are the number of vehicles owned and each vehicle's time of availability and geographic coordinates. A vehicle's availability time was considered to be the end time of the previous trip if it ends at home. Trip end times are approximated using the regional traffic assignment model described in Section 3.2. Hourly travel times were estimated for average driving routes between the 1552 TAZs, and were then added to the start times for each trip in order to approximate trip end times. In a second step, an array was created for each household that had a number of elements equal to the number of vehicles owned. Each vehicle in the array was initialized at the household's geographic coordinates. An algorithm then ordered all household trips chronologically and assigned every trip an index based on vehicle availability (time and geographic coordinates). Finally, each vehicle index was randomly allocated a vehicle type and model year based on the cumulative distribution function of the vehicle fleet composition of the household's residential area. Therefore, every driving trip in the OD survey was allocated a vehicle type and model year that remained constant over a day's worth of trip chains.

3.4 Running Emissions Model

Linked with the regional traffic assignment model, an emission processor was developed that incorporated the two main data sources described in Section 3.1 (OD survey data, vehicle registry) with two additional data sources as inputs (paths array, EF look-up tables). Two outputs were obtained, the individual running emission level for each individual trip and hourly link-level emissions for all roads in the regional network. The processor goes through the list of individuals in the OD survey and randomly selects a path for each trip based on the cumulative path volume distribution from the path array. For each link along the path, based on the link type, average speed, and vehicle type/age, it attaches an EF in g/veh.km, and finally, multiplies the EF by the length of the link. After generating an emission per individual trip, total emissions per person are

aggregated and assigned to the TAZ where the individual resides. We also calculate total emissions occurring on the network in each TAZ.

Four main databases are used to calculate individual trip emissions, these include: 1) the OD trip table, 2) the vehicle ownership database, 3) the paths array, and 4) the EF look-up table. The OD trip table and the vehicle ownership database are covered previously in Section 3.1.

Path Arrays

The path array output from the regional traffic model contains information on each path between every active OD pair. Every path in the array has information on the volume of vehicles for that path as well as the type, length, speed, and volume of each link along the path. A path was allocated to each driver based on their origin and destination TAZs. In the case of multiple paths for one OD pair, a path was randomly allocated based on the volume proportion between the multiple paths.

Vehicle EFs

Vehicle EFs were generated using MOVES. All default input distributions within MOVES were replaced with Montreal-specific data reflecting the vehicle fleet, fuel composition, and ambient conditions. These EFs (in g/veh.km) vary by vehicle type (PC and PT), age (30 model years), fuel (gasoline), average speed (15 speed bins ranging from 2.5mph to >65mph), season (winter, summer), and facility type (uninterrupted, interrupted). The latter is based on MOVES' differentiation between two different driving behaviors based on two different types of road facilities. Uninterrupted facilities are roadways that have controlled access points with no signal control (i.e. expressways), resulting in more free-flowing traffic. Interrupted facilities, on the other hand, are roadways with intersections, signal lights, or stop signs, resulting in more stop-and-go driving. The ambient environmental data applied to the summer and winter scenarios are highlighted in the next section. Emissions are computed for NO_x, HC, and greenhouse gases (as $CO_{2\text{-eq}}$). This leads to a large multi-dimensional look-up table with 10,800 EFs. Following the generation of the look-up table, trip

emissions (in grams) are calculated by matching the corresponding EF (g/veh.km) with each link along the trip taking into account vehicle characteristics and multiplying by the length of the link (km). EFs for link speeds that fall in between two speed bins are linearly interpolated. Further, emissions for each path are multiplied by the trip expansion factor and then assigned to the TAZ of the driver's home location, as well as allocated onto the TAZs of every link on the driver's path.

3.5 Start Emissions Model

In order to estimate trip-level start emissions, the emission processor required that each trip needed to have a soak-time and a vehicle-specific start EF. Soak-times were estimated once the vehicle allocation process was completed. The entire trip chain was tracked for every vehicle during the day and a sequence of engine ignitions and shutdowns was used to calculate soak-times. Specifically, the soak-time for a given trip is calculated as the start time of the current trip minus the end time of the previous trip. The maximum soak-time was capped at 1440 minutes (24 hours), and if a vehicle only had one trip in its trip-chain then it was given the maximum soak-time. The vehicle-specific start EFs were generated using the same platform (MOVES) as the running emissions with a similar Montreal-specific context. EFs for HC were generated; a total of 960 start EFs were computed in order to consider the effect of soak-time (8 bins), weather (2 seasons), vehicle type (2 types), vehicle model year (30 model years) and pollutant type (HC) independently. Given that Montreal has significant seasonal variability and that meteorological conditions can have a significant effect on start emissions, we simulated EFs for both a summer and winter scenario (Table 1).

Table 1 – Atmospheric Conditions Used For Emission Modeling

Season	Date	Temperature (^{o}C)	Atmospheric Pressure (kPA)	Relative Humidity
Winter	31-01-2008	-6.5	101	88
Summer	14-06-2008	21.1	101	60

Source : http://climate.weatheroffice.gc.ca/

EFs for vehicle model years between 1978 and 2008 were generated for PCs and PTs independently. As seen in Figure 6, increased vehicle age is associated with increased start emissions. A similar relationship is observed for all pollutants and atmospheric conditions considered. Vehicles manufactured before 1985 are associated with considerably higher start EFs. It is also interesting to note that the jump in start emissions for PTs coincides with the significant increase in SUV and minivan popularity during the mid- to late-1990s.

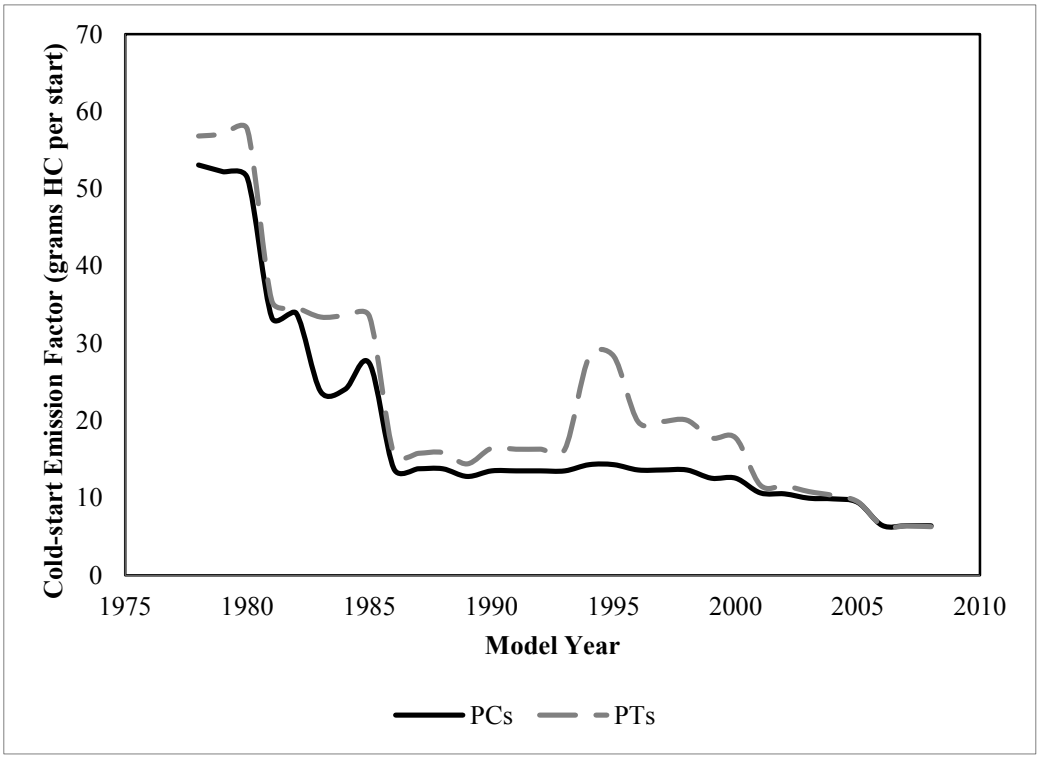

Figure 6 – Start emissions for vehicle types and model years under winter conditions

Start EFs were developed for eight different soak-time bins in line with the eight operating modes used for start emission calculations in MOVES. The eight operating modes corresponded to the following time bins (ranges in minutes): (1) 0-6; (2) 7-30; (3) 31-60; (4) 61-90; (5) 91-120; (6) 121-360; (7) 361-720; and (8) 721-1440. The relationship between soak times and EFs is nearly logarithmic (Figure 7) and compares well to previous findings into the connection between start EFs and soak-times (Favez et al., 2009). Engine starts with soak-times greater than 12 hours (720 minutes) are considered to be cold-starts. Trip-level start emissions were estimated through the emission processor by assigning a start EF to each vehicle/trip based on its soak-time bin and vehicle characteristics (type and model year). The trip-level start emissions from the OD survey were then expanded to the full population based on survey expansion factors to produce total daily start emissions. In addition, hourly start emissions along with their spatial distributions are estimated.

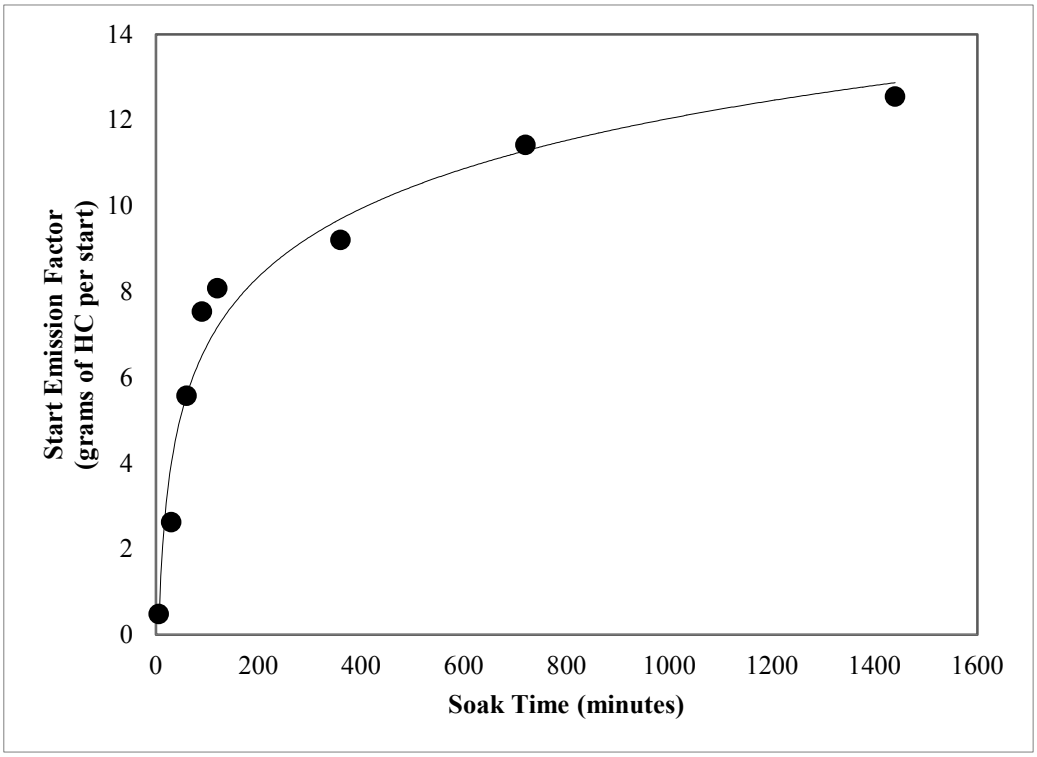

Figure 7 – Start emissions for PCs (model year 2000) as a function of soak time under winter conditions

3.6 Model Validation

Transport Model

The regional traffic assignment model was validated using traffic counts (integrated over a week) on 75 major arterials within the region as well as five bridges linking the Island of Montreal with the rest of the region (one count for each direction). The data were obtained using automatic and manual traffic counts conducted by the city of Montreal between the years 2008 and 2012, and the total number of count points was 160. The comparison between actual counts versus predicted counts provides an R^2 value for the 6AM - 7AM period of 0.78 (Figure 8) and a R^2 value for the 7AM - 8AM period of 0.65 (Figure 9). The correlations (R-values) for the remaining 24-hour periods range from 0.62 to 0.86. Currently, traffic counts on highways remain unavailable to the research team and hence validation was confined to arterial roads and bridges. We recognize this as a significant limitation that will be addressed once highway traffic counts are obtained. However, given the strong correlations across the 24-hour period, we can confidently state that the model is adequately capturing the regional travel behaviour.

As mentioned earlier, a large portion of the MMR includes the Montreal Island which is heavily dependent on its bridges. To validate our MMR model we also examine simulated traffic volumes across the day on Montreal bridges (Figure 10).

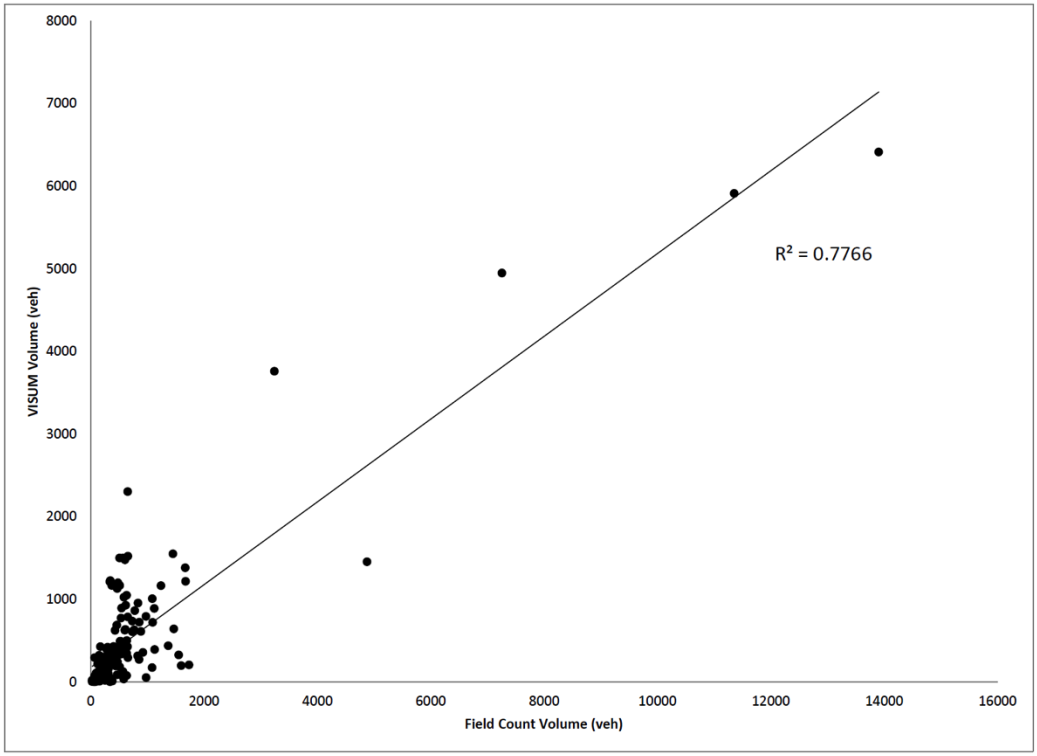

Figure 8 – Comparison between measured and modelled traffic volumes (6 - 7 AM)

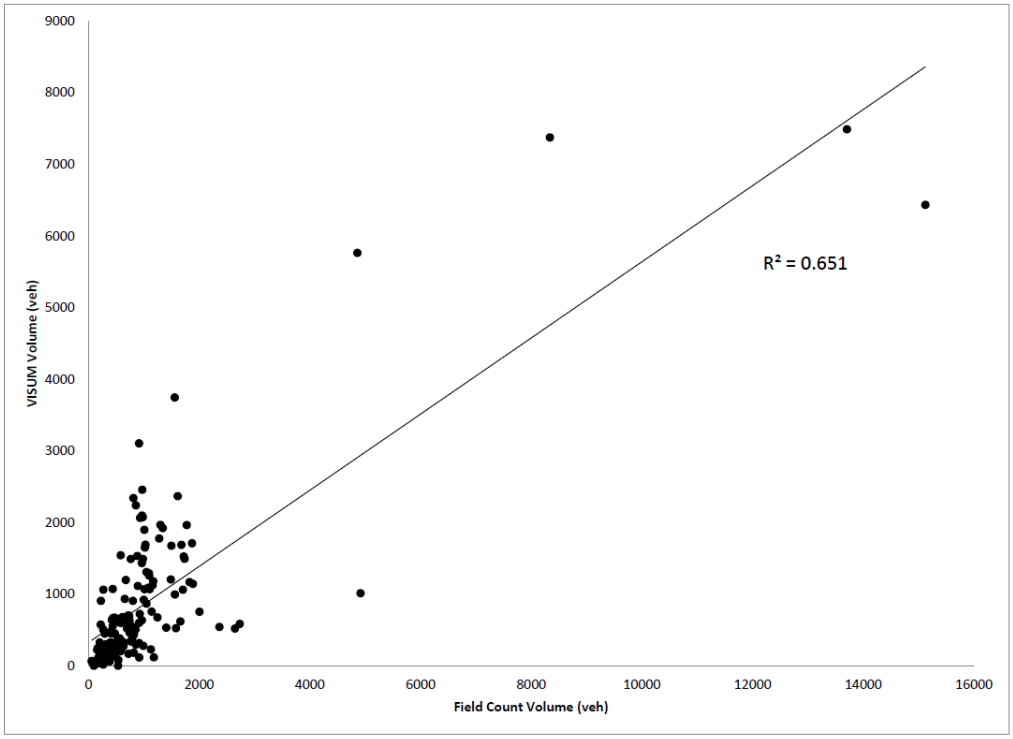

Figure 9 – Comparison between measured and modelled traffic volumes (7 - 8 AM)

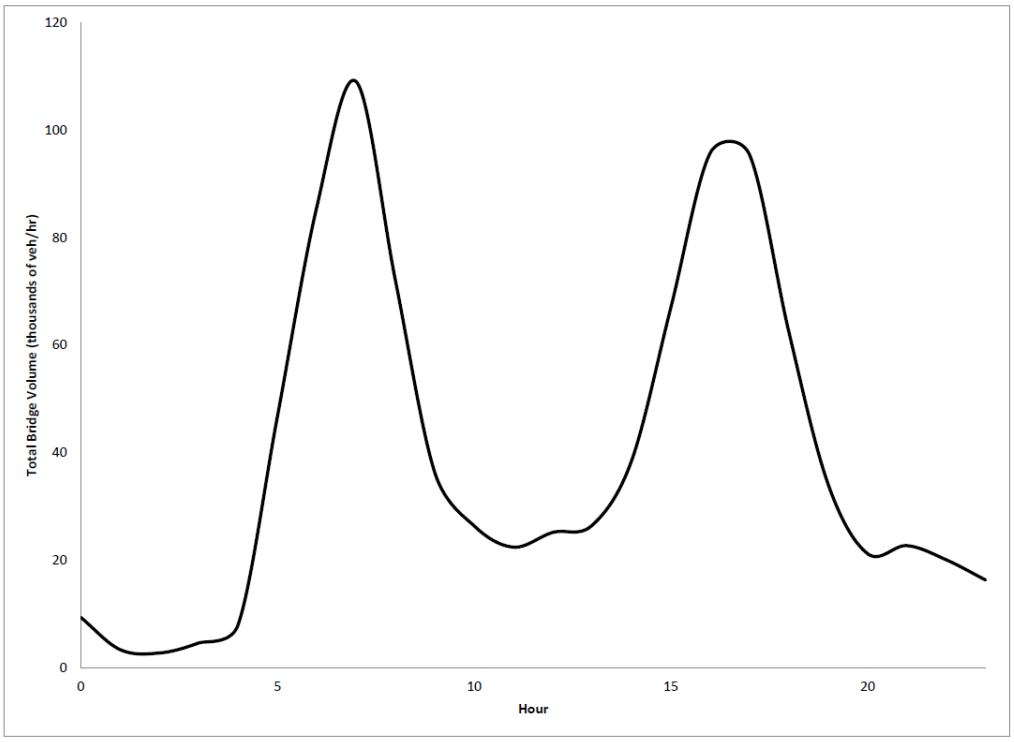

Figure 10 – Hourly traffic volume profile on the bridges

Emissions Model

Initially, attempts were made to validate the emission results by comparing regional daily GHG emission estimates across several Canadian metropolitan regions (Table 2). Each estimate incorporates all private vehicle travel (PCs and PTs) from a standard workday, and measures GHG levels as $CO_{2\text{-eq}}$ emissions. The comparison includes two estimates for Montreal from varying years and geographic boundaries, as well as two from the Toronto area and another from Metro-Vancouver. Despite the difficulties in assessing inventories across different regional sizes, estimate years, and methodologies, the results are still relatively similar especially compared to the previous Montreal-based estimates. The one outlier from Hao et al (2007), with estimates over two-times greater, is expected given that the Greater Toronto and Hamilton Area is over two-times the size of the MMR.

Table 2 – Comparison of Daily GHG Emission Inventories from Private Vehicle Operation

Region	Source	Year of Estimate	GHG Estimate (tons per day)
MMR	Integrated transport and emission model	2008	11,920
Montreal CMA	Statistics Canada (2012)	2007	11,900 – 14,500 [a]
Island of Montreal	Logé (2006)	2003	10,070 – 12,790 [a]
City of Toronto	ICF International (2007)	2004	17,040 – 20,690 [a]
Greater Toronto & Hamilton Area	Hao et al. (2007)	2001	24,120 – 25,810
Metro Vancouver	BC MoE (2013)	2010	10,600 – 12,872 [a]

[a] Calculated from a yearly estimate by assuming 261 workdays per year and that 70-85% of traffic occurs during the week

While it is hard to validate link-level NO_x emissions at a regional level, we propose to validate our link-level NO_x emissions (in grams) by evaluating their association with near-road NO_2 levels (in parts per billion) derived previously. For this purpose, the NO_x concentrations estimated at the TAZ level (grams per km^2) are compared to ambient NO_2 concentrations from a land-use regression (LUR) model developed previously for the island of Montreal. The LUR model was created by Crouse et al (2009a) through a series of dense air quality monitoring campaigns whereby NO_2 samplers were placed at 133 near-roadway points at a height of 2.5 meters. Data on land-use and road density were then obtained for all locations, and a resulting multivariate regression model was estimated and used to predict NO_2 concentrations in areas without measurements.

The resulting overlay between link-level NO_x emissions and NO_2 levels is presented in Figure 6. Based on the number of raster cells falling in each TAZ, we calculate the average NO_2 level (in ppb) per TAZ and correlate this level with the level of NO_x emissions occurring in the same TAZ per km^2. While the aggregation to the level of the TAZ is expected to introduce disparity in the two datasets

(therefore reducing the correlation coefficient), a visual inspection of Figure 6 clearly indicates that our highest simulated NO_x emissions do correspond to the areas with the highest NO_2 levels in Montreal. Furthermore, we observe that the overall correlation between our NO_x link emissions and NO_2 concentrations along roadways is around 0.8.

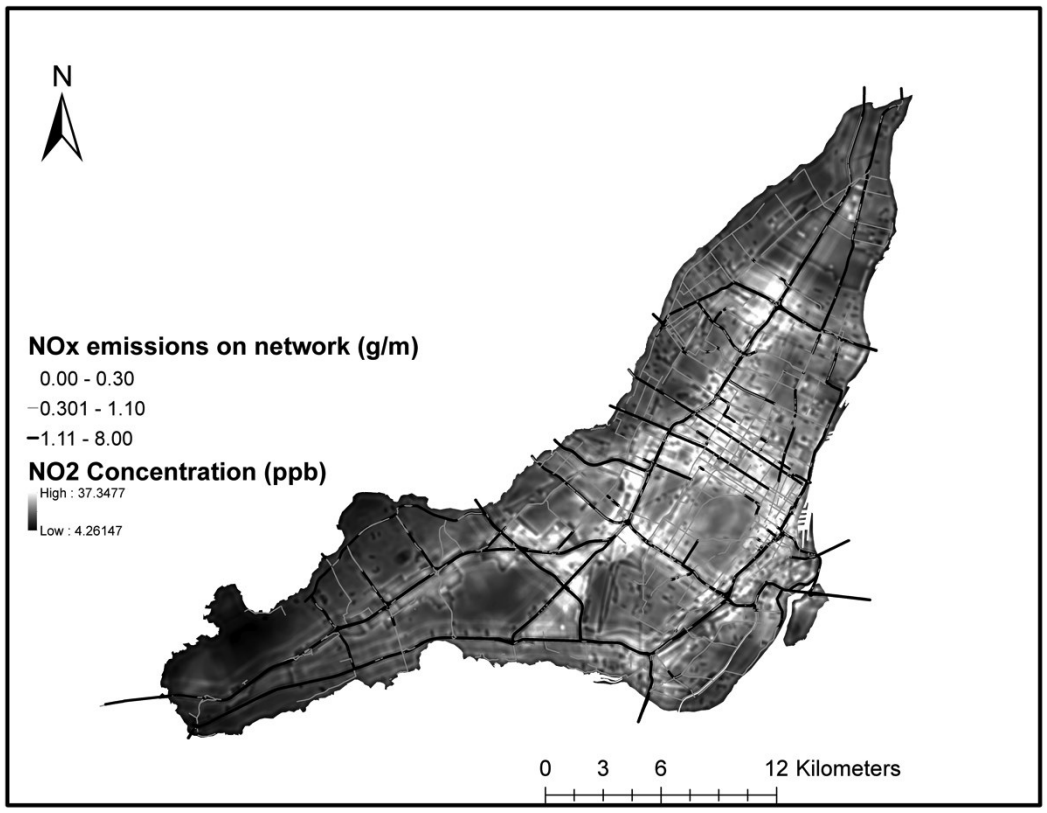

Figure 11 – Link-level NO_x emissions overlaid on a map of ambient NO_2

CHAPTER 4:
EVALUATING THE VARIABILITY IN EMISSION INVENTORIES

4.1 Context

The importance of accurate emission inventories has never been greater given the current impact that transportation systems have on the local and global environment, highlighted in Section 1.1. The current state of practice in research primarily involves the estimation of inventories through integrated traffic and emission models. Increases in model complexity have generally resulted in improved estimates, yet the improvements often come at the cost of investing in resource-intensive data inputs. In addition, not all investments in more accurate data inputs yield similar increases in estimate accuracies. For the research sector, this may not be a significant issue, yet for primary practitioners (ie. metropolitan planning agencies, provincial/state governments, etc.) involved in environmental and public health policy, this becomes much more relevant.

Input data are often either non-existent or resource- and time-intensive to gather, therefore simplifying assumptions must be made. Yet which simplifying assumptions are reasonable, and which result in estimation errors, is still not entirely known. Previous literature reveals two main studies in the past decade that have attempted a comprehensive review of best practices in emission modeling. Kioutsioukis et al. (2004) were the first in assessing the uncertainty and sensitivity of emission models of the late 1990s and early 2000s. Their summary of previous research concluded that accurate activity data was as important as accurate emissions data in generating better emission inventories, and that sensitivity analysis must also be added to all emission models. More recently, Smit et al. (2010) performed a review and meta-analysis of integrated traffic and emission models, specifically concerning validation techniques. They had a similar finding in that there was an inadequate understanding of uncertainties in traffic emission models. Furthermore, they concluded that there was likely a modeling optimum that would balance input accuracy and model accuracy. This optimum point is characterized by diminishing marginal returns in model accuracy if more

resources are invested in input accuracy, and vice versa. Model development, ie. which details to focus on, and model application, ie. which data is most relevant to collect, were put forward as two key elements in establishing a modeling optimum.

This chapter aims to explore the different input elements within an integrated transport and emission model and identify those that contribute the most to the accuracy of the final emission inventory. For this purpose, we estimate total daily HC emissions from passenger travel at the metropolitan level through the integrated modeling framework described in Section 3. The primary inputs of both running and start emission models are then altered in order to test the effects of different levels of aggregation in model inputs on the final estimates. We also test the effects of prevailing assumptions frequently made when emission inventories are conducted within government agencies.

4.2 Methodology

With the development of the integrated traffic assignment and emission model, a series of model runs were then undertaken in order to systematically evaluate the effects of input data precision on the final emission inventory. In addition, the effect of randomness we built into the model and which pertains to the vehicle allocation as well as path allocation processes is evaluated through multiple model runs leading to the generation of a standard error associated with every daily regional emission estimate.

A total of 7 sets of model inputs were varied; these include: 1) the inclusion or exclusion of start emissions; 2) ambient temperature (winter vs. summer); 3) level of speed aggregation extracted from the assignment model (average network speed, trip speed, link speed); 4) vehicle age distribution (average vehicle age in the province vs. real distribution obtained from registry data); 5) vehicle types distribution (assuming all PCs vs. real distribution obtained from registry data); 6) soak-time distribution (assuming all starts are cold starts, assuming that all starts

are warm starts, using default soak time distributions, and deriving the real soak time distribution from trip start and end times); and 7) path selection (shortest path or stochastic assignment).

1) Inclusion of start emissions – Excess emissions during engine starts have been estimated to account for nearly 28-31 percent of total on-road VOC emissions under summer conditions (Borrego et al., 2004; Houk, 2004). Kioutsioukis et al. (2004) also found that cold start effects in relation to average trip lengths were one of the three most important elements in accurate VOC estimates. While earlier emission inventories have accounted for starts through three different types of running EFs (cold-transient, hot-transient, and hot-stabilized), the current generation of emission simulators tend to separate running and start EFs. Therefore, in order to evaluate the effect of start emissions on daily regional emission inventories in isolation from other factors, we ran the model while including and excluding start emissions.

2) Season – For regions and urban areas with high temperature differentials between summer and winter, season becomes an important consideration in developing emission inventories. Emission rates, especially the excess ones from starts, tend to significantly change under winter conditions, with start contributions rising to over 50 percent of total on-road emissions (Houk, 2004). Therefore, total emissions (start and running) were evaluated under summer and winter conditions in order to assess the isolated effect of ambient temperature.

3) Travel speed – There are varying levels of detail with regard to travel speed aggregations used in emission modeling. The simplest assumption involves applying the average network speed (daily or peak-period) to all trips (Ko et al., 2011; Brand and Preston, 2010). Certain models have increased the level of detail by assuming average trip speeds for emission calculations (Borge et al., 2012; Barla et al., 2011; Frank et al., 2000; Hao et al. 2000). Adding another layer of detail, the majority of emission models tend to use average link-speeds (Borge et

al., 2012; Hao et al., 2010; Beckx et al., 2009a; Xia and Shao, 2005; Borrego et al., 2004; Anderson et al., 1996). The detail in travel speed has been repeatedly shown to be highly significant with regards to emission estimates. Smit (2006) concluded that congestion and its impact on travel speeds was the second most important element in HC estimates after VKT. Anderson et al. (1996) found that HC estimates increased by 56 percent when using congested versus free-flow speeds. Therefore, three different travel speed assumptions were tested. The first was the most detailed and involved estimating link emissions using the congested speed of every link in a trip's path. The second involved calculating an average trip speed for every OD trip using the trip length and time, and then estimating link emissions using this speed. The third speed assumption was to apply an hourly network-wide average speed to each link/trip.

4) Vehicle age – Vehicle age is a significant factor in emission modeling. Previous studies have made three common assumptions: (1) all trips use the same vehicle age (Ko et al., 2011; Hao et al., 2000); (2) all trips are assigned a single EF representing the actual distribution of vehicles (obtained from fleet registry data; Borge et al., 2012; Xia and Shao, 2005; Borrego et al., 2004; Frank et al., 2000; Anderson et al., 1996); or (3) each trip is allocated a model year that is related to a unique EF (Barla et al., 2011; Hao et al., 2010; Brand and Preston, 2010). Therefore for this study two different vehicle age assumptions were tested. One involved creating a set of EFs from Montreal-specific fleet information for 30 different model years (1978-2008). When each trip was assigned a unique vehicle age, it was also associated with a single EF for that same model year. The second involved using an EF for one model year, and assuming that all trips were made using that same vehicle age. The vehicle age used was the average for the Montreal fleet, which is eight years old (model year 2000 in 2008, the year of our simulation).

5) Vehicle type – Common misconceptions in operational emission modeling frameworks is to assume that all household vehicles are of the same type, often

assumed to be PCs (Ko et al., 2011; Brand and Preston, 2010; Anderson et al., 1996). For this reason, we evaluated the effects of two different vehicle type distributions: a) the actual household vehicle types existing in Montreal including PCs, and PTs, a category that covers light-duty trucks and sports utility vehicles; and b) the assumption that every trip was made using a PC.

6) Soak-time – The time between turning an engine off and its successful re-ignition is known as the vehicle soak-time, and is a primary determinant of start emissions. Previous generations of emission models employed default soak-time distributions in order to account for start emissions. Over a certain period, all the trips would be randomly allocated soak-times based on that hour's distribution. Nair et al. (2000) recommended replacing the default distribution with regional-specific data if possible. For this study, individual soak-times for each vehicle/trip were estimated based on the vehicle allocation algorithm. Three other soak-time configurations were also tested for the start emissions analysis. The second and third involved the assumptions that every start was a cold start (largest soak-time bin), or a warm start (smallest soak-time bin). The fourth configuration is based on the assumption that all vehicles in the survey data are randomly assigned a soak-time based on default cumulative distributions from MOBILE6 (USEPA, 1998). The MOBILE series is the previous generation of emission models developed by the USEPA, with MOVES being its successor. Given that numerous studies have used either MOBILE6 (Hao et al., 2010) or a previous generation of the MOBILE model (Frank et al., 2000; Anderson et al., 1996), it is interesting to assess its impact compared to emission estimates generated from locally derived soak-times. The comparison between soak-time distributions derived from local travel diaries in Montreal (for 2008) and from MOBILE6 is illustrated in Figure 12. The differences across several hours seem to be relatively consistent between the MOBILE6 distribution and the travel diary distribution, however the overall differences between the two distributions are fairly large. The travel-diary distribution favours larger soak-times (greater than 12 hours), whereas the MOBILE6 distribution has a more relatively balanced range. Initially, this

suggests that the MOBILE6 soak-time distribution might underestimate the total start emissions given that the soak-times are smaller on average.

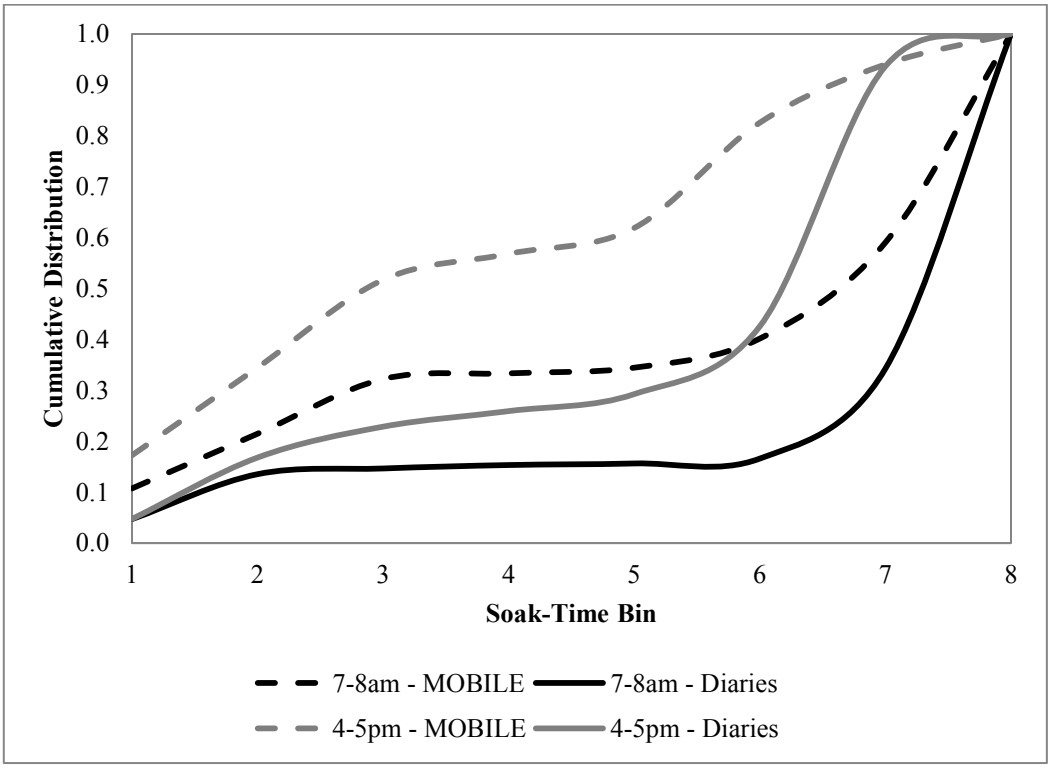

Figure 12 – Soak-time comparison between local travel diary information and MOBILE6 defaults

7) Path selection – Not to be confused with path allocation (where vehicles are allocated to different paths linking their origin and destination based on volume distributions on each path resulting from the traffic assignment), path selection involves the choice of path used for any trip between an OD pair that is determined by the assignment type employed in the regional traffic model. Various assignment types used in conjunction with emission models include: (1) shortest path (Barla et al., 2011); (2) deterministic user equilibrium (Beckx et al., 2009a; Borrego et al., 2004; Anderson et al., 1996); (3) stochastic user equilibrium (Hao et al., 2010); and (4) dynamic user equilibrium (Borge et al., 2012; Xia and Shao, 2005). Otherwise, VKT data are sometimes gathered directly from travel surveys (Ko et al., 2011; Brand and Preston, 2010; Frank et al., 2000; Hao et al., 2000). For computational reasons, both deterministic and dynamic user

equilibrium assignments were ignored in this study, resulting in two path selection algorithms being tested. One involves a stochastic path selection, which randomly allocates a trip to a path within a probability-based path set for every OD pair. The other involves the simplification that all trips select the shortest path.

The final element of interest in the framework is the variance within the emission processor. Assuming all other inputs remain constant, the variance within the emission output is caused by randomness in both the vehicle allocation and the path allocation steps. The vehicle allocation step entails randomly assigning each vehicle a model year and type based on the cumulative vehicle fleet distribution characterizing the household's residential zone. The cumulative distribution function was created using vehicle registry data, broken down into number of vehicles owned by type and model year. Therefore, the individual vehicles change between model runs, however the aggregate makeup of each zone remains consistent with the actual fleet distribution. Meanwhile, the path allocation step entails randomly assigning a trip to a certain path between its origin and destination TAZs based on a cumulative path volume distribution function. The cumulative distribution function is created for every path set and is based on the volumes assigned to each path from the regional traffic assignment model. Therefore, individuals will have a higher chance of taking the most popular (ie. least congested) paths, yet there are lengthier alternatives also available.

In order to account for this variance, the model was run under three different vehicle allocation simulations as well as three different path allocations combined to create three model iterations. These three iterations will form the basis for error estimation, and every input (belonging to the seven categories presented) is evaluated three times thus leading to three values for the total emissions output. The three values are averaged and a standard error (SE) is calculated, totaling 27 total model runs and an additional 12 runs of the start emissions processor to assess soak-times. Figure 13 details the process used in testing five sets of data input, with each tree being generated for both seasons of analysis (soak-time is

omitted from the results tree since it uniquely effects start emissions). The results are presented in the same format with the mean and SE from the three iterations for each inventory estimated.

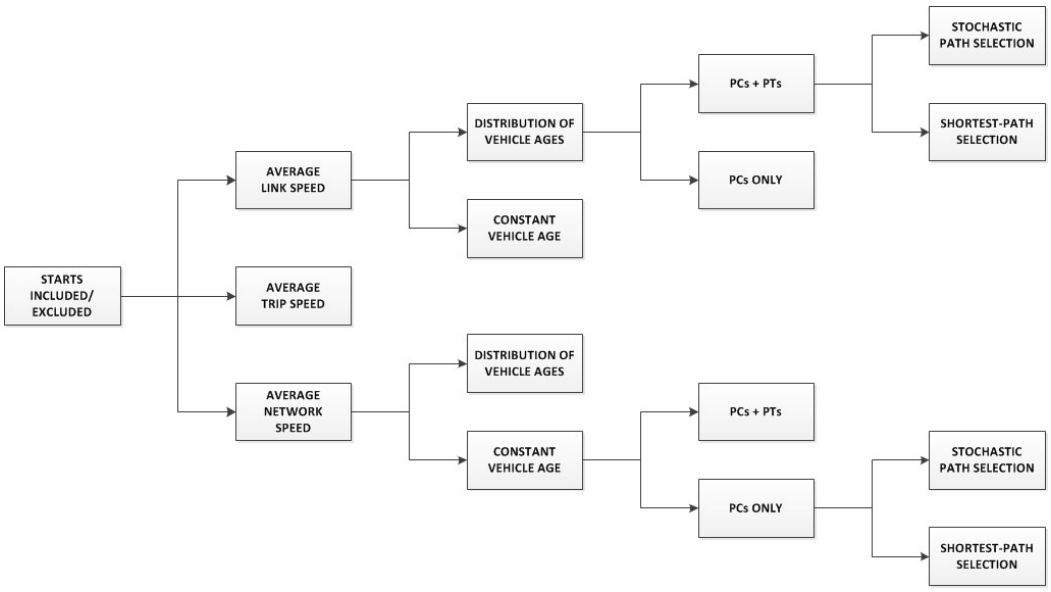

Figure 13 – Flowchart of changes to data inputs and model simulations

4.3 Results

Results of all the data input permutations that were tested are presented in the two trees that show daily regional emission estimates in tons per day, along with SE values (Figure 14). The two trees serve to differentiate two sets of emission models with one involving a common omission: start-emissions. The figure shows an estimate that includes start emissions (top tree) versus a less accurate one that ignores starts (bottom tree). The uppermost branch of the top tree reveals the most detailed emission estimate of about 18 tons per day, a quantity comparable to previously estimated daily HC inventories for similar Canadian metropolitan areas (Hao et al., 2010; Anderson et al., 1996). Meanwhile, it is important to note that the SE of all estimates is due to randomness in the vehicle and path allocation steps and accounts for at most 0.36 percent of the daily regional emission estimate. This means that the variance in allocating vehicles to individual trips based on zone-level registry data is insignificant given the size of the region and

the fact that we are only looking at total daily emissions. More specifically, vehicle ownership trends (type and age) at the zonal level are respected during each iteration resulting in relatively consistent emission estimates, even though vehicle allocation at the individual level may be varying drastically. The same conclusion can be reached for the randomness due to the path allocation process. Individuals are likely taking different paths over different iterations, however at the aggregate level the variance is small. These results are contrasted with the substantial inaccuracy when solely making assumptions based on vehicle ownership data. For instance, estimates involving a simplification in vehicle age actually result in overestimations of 4 to 32 percent. Larger overestimations occur in scenarios where start emissions are included, owing to the fact that they are highly dependent on vehicle age (Figure 6).

Figure 14 also highlights the impact of various assumptions in combination. For instance, the lowest branch of the lower tree shows the multiplying effect of simplifications regarding start-exclusion, speed aggregation, vehicle type and age, and path selection. Together, those impacts lead to an underestimation of 28 percent compared to the detailed estimate excluding starts, and an underestimation of 76 percent compared to the most accurate estimate including starts. However, making all those assumptions while including starts results in an underestimate of 7 percent.

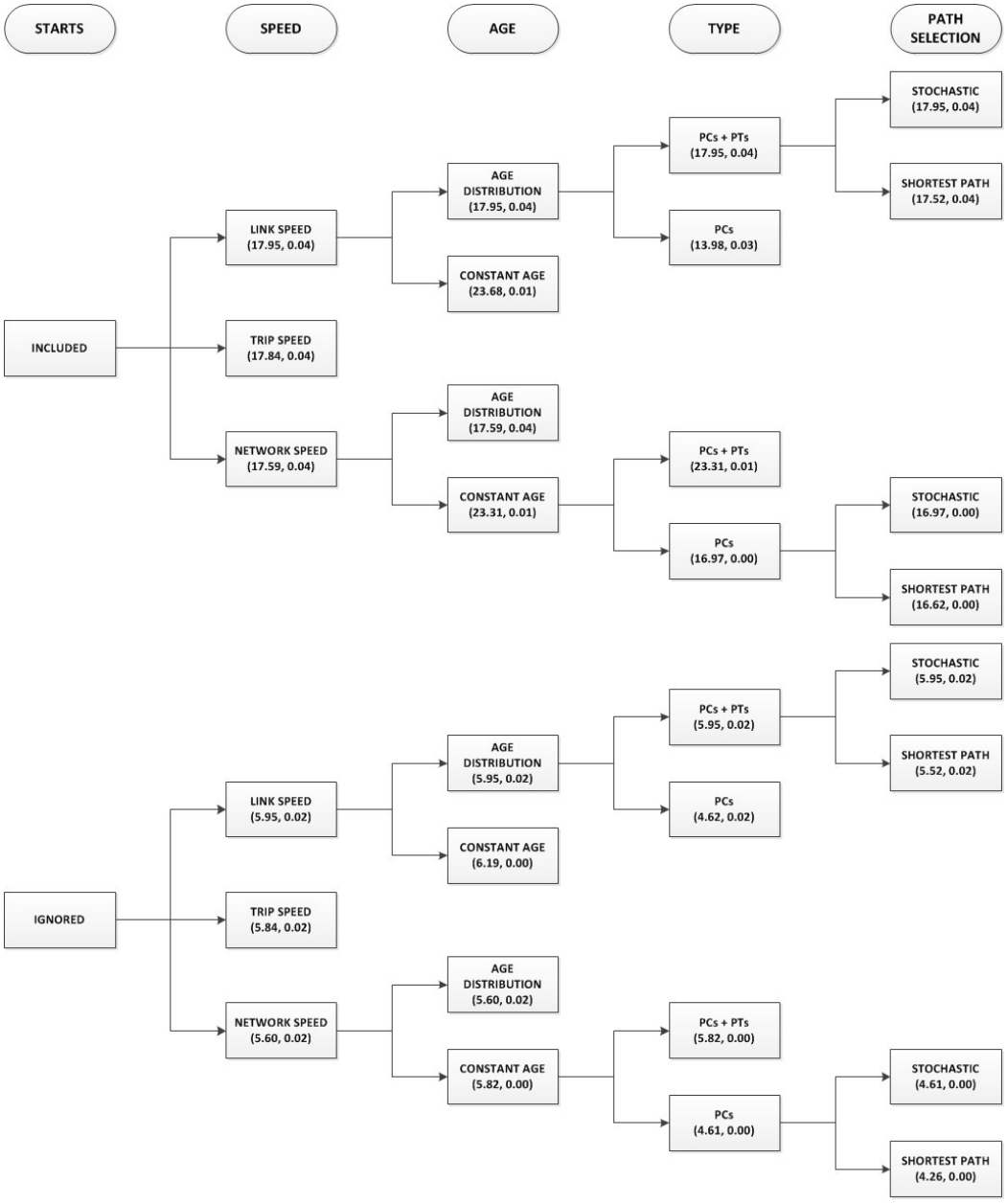

Figure 14 – Sensitivity results for daily regional emission estimates (values in parentheses include daily mean HC amount followed by its SE)

Analyzing the effect that starts have on daily estimates, it is clear that ignoring start emissions will result in significant underestimations. Daily regional emission estimates increase threefold when including starts under summer conditions and this increase can rise to as much as eight times if winter conditions are considered (Figure 15). These results show that starts alone can contribute 67 to 86 percent of total daily HC emissions, percentages that are twice as large as those suggested in

previous research (Borrego et al., 2004; Houk, 2004). These results also highlight two important points with regards to season, in that: 1) substantial differences in weather conditions do not have a significant effect on running emissions, at least for HCs; and 2) that any impact seasonality has on running estimates pales in comparison to its pivotal role in start estimates.

Meanwhile, the effect of different assumptions on travel speed aggregation is summarized in Figure 16. The effect of using average trip speeds in emission calculations reduces the total daily estimate by 2 percent from the baseline, which employs more accurate average link speed data. Applying the more simplistic assumption that all drivers travel at average hourly network speeds also results in an underestimation of about 6 percent. The fact that both simplifications result in underestimation comes as no surprise given that congestion effects tend to be lost in speed aggregation. However, the impacts are much smaller than anticipated. This is possibly caused by aggregating hourly running emissions, which typically vary significantly in peak versus non-peak traffic, into one daily estimate. Yet hourly emissions from all three speed inputs were compared and no significant differences between the aggregations were observed over the 24-hr period. The reasons for this are likely twofold: 1) the EFs are not that sensitive to speeds since instantaneous second-by-second speeds are not simulated, and 2) the speed impacts are negated by the sheer magnitude of regional VKT.

Regarding the co-impacts of vehicle age, the assumption that all trips are made with an average model year (8 years old) results in a consistent overestimation of about 4 percent across each of the speed aggregation scenarios. The error bars in Figure 16 represent the range of estimate totals from model randomness. The smaller error bars of the constant vehicle age scenarios clearly indicate that the bulk of model randomness lies in the vehicle allocation step.

If the effect of vehicle type in combination with vehicle age is then isolated, the resulting outputs show that assuming all trips are made with PCs leads to a large

underestimation in emission estimates (Figure 17). The underestimate from this assumption is nearly 25 percent and is consistent whether applying the full fleet age distribution or assuming an average vehicle age. Similarly when including starts, the underestimation is 22 percent. This indicates that vehicle type has a much larger impact than vehicle age on estimate accuracy. In addition, the size of the error bars in Figure 17 again highlight that model randomness is largely due to variance in vehicle allocation.

Moreover, the type of path selection algorithm employed in the transportation model has a significant impact on the daily emission estimate. The assumption that all trips were taken on the shortest path results in a 7 percent drop in total regional emissions from the baseline, in which a path set is created through a stochastic distribution (Figure 14).

The results of analyzing the effects of soak time on starts can be seen in Figure 18. The error bars shown represent the range in values from different vehicle allocations. The soak-time distribution from detailed travel diaries estimated 12.00 tons of start-based HCs. Assuming all trips began under warm-start conditions resulted in a drastic decrease of 94 percent, whereas the total start emissions rose by 33 percent under the assumption that all trips were cold-starts. Given that start emissions are responsible for the majority of total HC emissions, it is important that soak-time distributions are accurate due to the wide range of values seen in Figure 18. Another finding of note is that the total daily start emission estimates are relatively similar when using the local soak-time distributions derived from travel diaries versus the default distribution in MOBILE6. Although the contribution from starts was higher under the soak-times derived from travel diaries (12 tons per day vs. 11.5 tons per day), the differences are smaller than expected (Figure 12). If hourly start emissions are compared, it is evident that the discrepancy in estimates is primarily due to differences in the morning and afternoon peak-periods (Figure 19). Meanwhile, the distributions from travel

diaries vs. MOBILE6 provide nearly identical start emission totals for all other times of day.

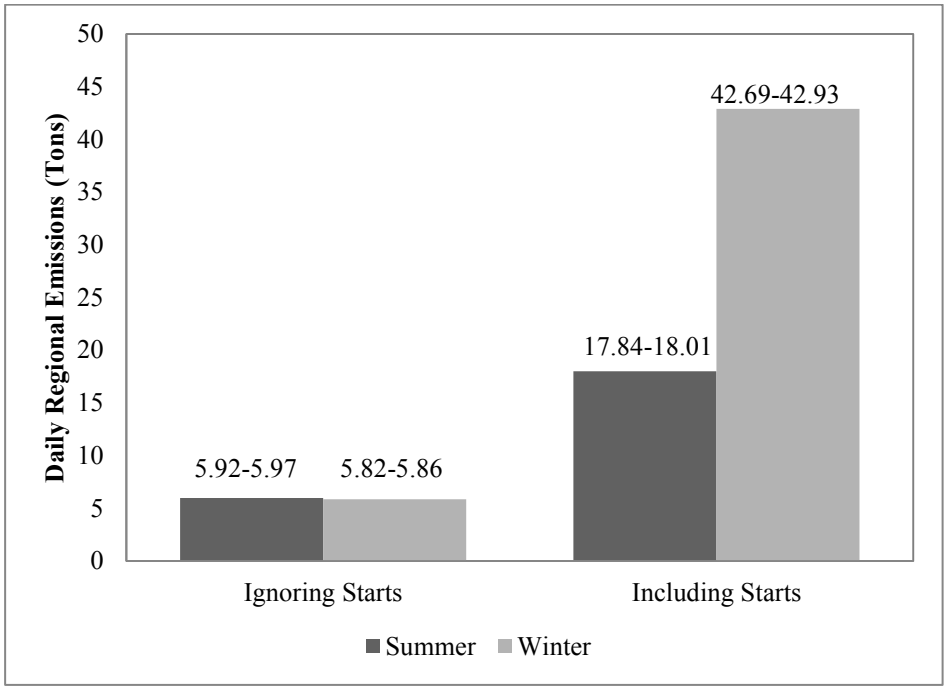

Figure 15 – Daily regional emissions ignoring and including the effect of starts and season

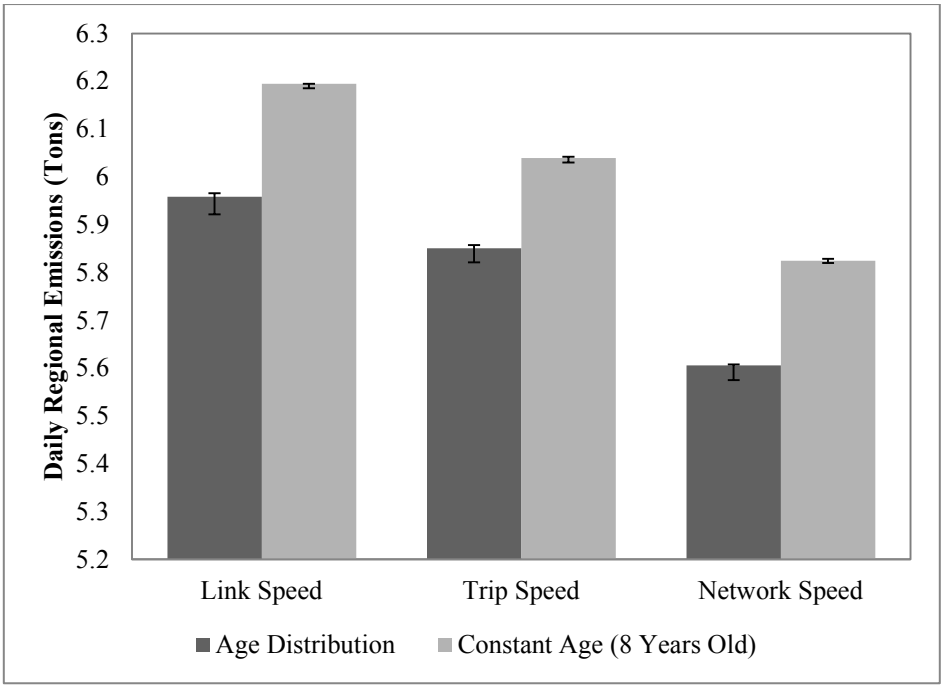

Figure 16 – Daily regional emissions for different travel speed aggregations and vehicle ages (ignoring starts)

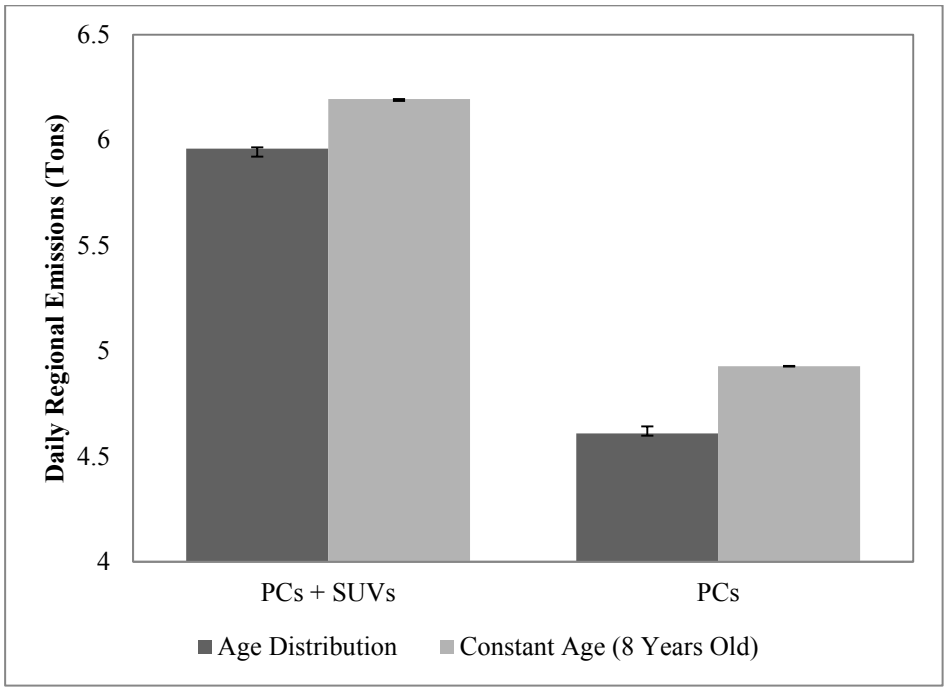

Figure 17 – Daily regional emissions for different vehicle ages and types (ignoring starts)

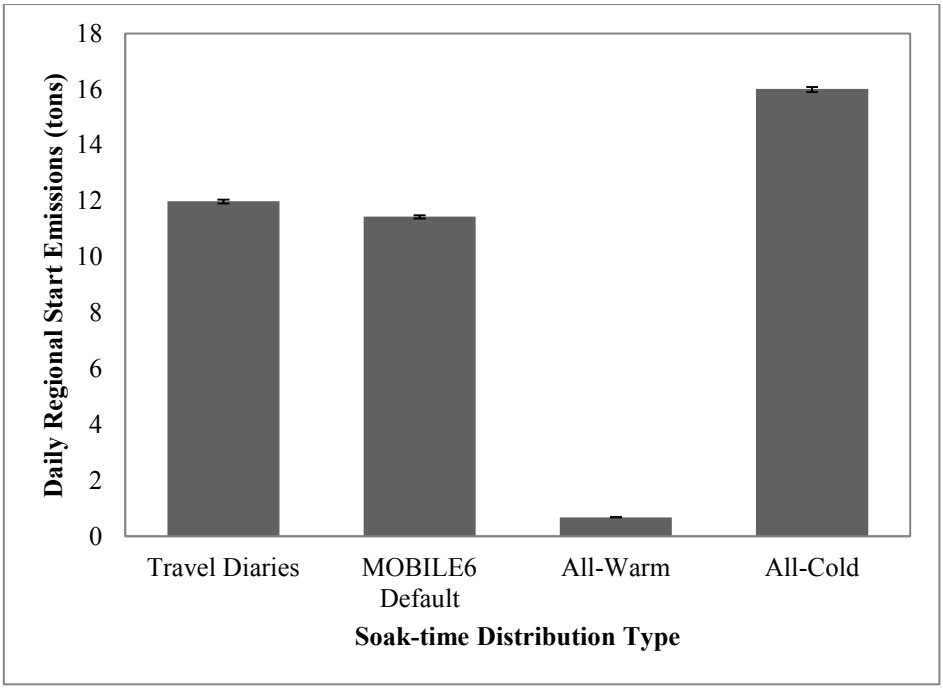

Figure 18 – Daily regional start emissions for different soak-time distributions

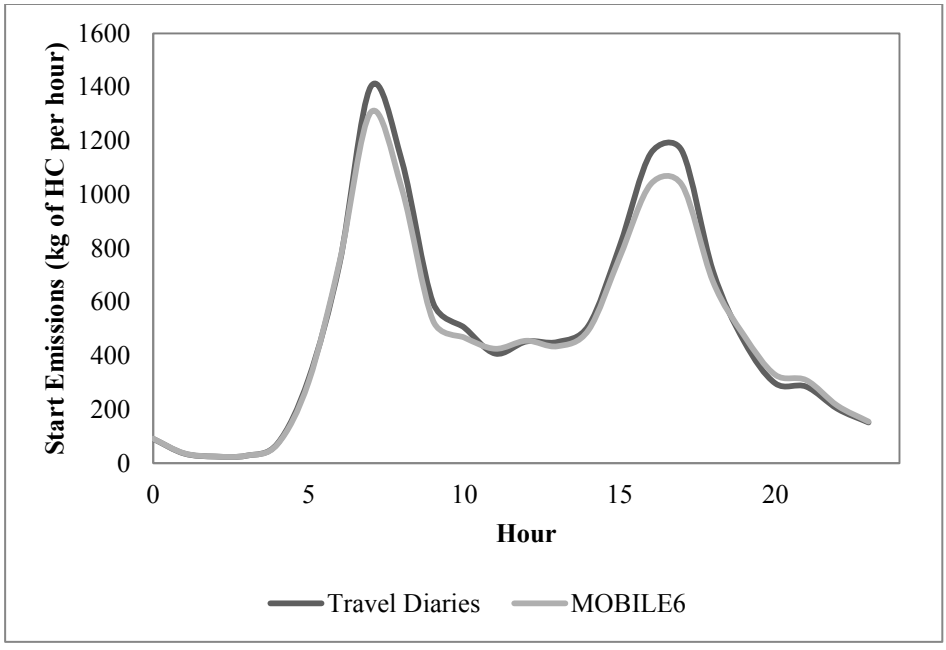

Figure 19 – Soak-time comparison of start emissions per hour

4.4 Conclusions

The level of accuracy in travel behaviour data is highly linked to accurate emission inventories (Kioutsioukis et al., 2004). Using accurate travel behaviour data as the baseline, the question remains as to which inputs contribute the most to the accuracy of emission estimates. To address this question, the integrated traffic and emission model was used to estimate daily regional emissions for the MMR. The detailed model was set as the baseline, and then seven different data inputs were altered in isolation, as well as several in combination, to assess their impact on daily emission inventories. Overall, start emissions had the largest impact. Even under summer conditions, start emissions are estimated to make up two thirds of total on-road HC emissions. The impact of starts would likely be less if inventories were being made for other pollutants such as NO_x. Vehicle registry data is the next element with the highest impact, specifically data on vehicle type distribution. SUVs and light-duty trucks emit more running and start emissions than PCs with similar model years, and so regions with high levels of PT use need to account for them. Meanwhile, speed aggregation and path selection type both have significant impacts on regional emission estimates, however nowhere close to the extent of including starts or accurate vehicle data. Our results also seem to support the argument that VKT remains a significant element in determining trip emissions. For practitioners, reaching the modeling optimum that balances input accuracy with model accuracy likely means investing resources in start emissions and accurate vehicle ownership data.

CHAPTER 5:
LAND-USE AND SOCIOECONOMICS AS DETERMINANTS OF TRAFFIC EMISSIONS AND INDIVIDUAL EXPOSURE TO AIR POLLUTION

5.1 Context

The objective of this chapter is to better understand the generation of traffic-related air pollution at a metropolitan scale and identify the regions that are potentially the most affected by these emissions. We propose two measures of traffic emissions that potentially capture inequity in the spatial distribution of emissions: (1) the average level of emissions generated per individual and (2) the level of emissions occurring in a zone as a proxy for air pollution exposure. These indicators are estimated at the TAZ level through the integrated transport and emission model. We examine the spatial distribution of emissions as well as capture the determinants of emissions generated and exposed to through a multivariate regression analysis of the two indicators against a set of land-use and socio-economic variables.

Using significantly more aggregate travel and emission modeling tools, a number of studies have calculated individual and household emissions (from transport only) at a metropolitan level and analyzed the relationship between emissions and a host of socio-economic, land-use and transport supply variables. In one of the earliest studies conducted in California, Khan (1998) found that richer households might have higher vehicle emissions because they drive more often and own more vehicles. Poorer households were likely to have higher emissions as well because of their older, higher polluting vehicles. Frank et al. (2000) explored the relationship between land use patterns and household vehicle emissions in the Puget Sound region and found that household density, work tract employment density, and street connectivity (block density) were inversely related to household vehicle emissions, while commute trip distance had a positive influence. More recently, Brand and Preston (2010) estimated CO_2 emissions at the individual level for the Oxfordshire region in the United Kingdom. They found

a significant relationship between individual CO_2 emissions and age, gender and car ownership. Income, household location, working status and accessibility were not found to be significant. In another study with a similar methodology focusing on the Seoul metropolis area, Ko et al. (2011) found that household location and income were significant in relation to individual CO_2 emissions, along with age and car ownership. Barla et al. (2011) observed similar effects in Quebec City.

5.2 Methodology

The emission post-processor estimates two indicators of traffic-related emissions: 1) an average level of emissions generated per person for each TAZ calculated by dividing the total emissions generated by residents of the TAZ with the TAZ's population. This measure is an indicator of the "polluting power" of the TAZ; and 2) an average level of emissions occurring in a TAZ calculated by dividing the total emissions allocated to that TAZ by its area (in km^2)[1]. This measure relates to the amount of pollution experienced by a TAZ; in this chapter we use it as a proxy for air pollution exposure in the absence of an air pollution dispersion model. In our analysis, we restrict ourselves to examining the NO_x related emissions[2] as they have the highest co-locational association with other traffic-related pollutants (Beckerman et al., 2008; Wheeler et al., 2008).

In order to capture the strengths of associations between vehicle emissions and land-use and socio-economic attributes, a regression analysis was performed on the two TAZ-level indicators: 1) average emissions generated per individual, 2) emissions exposed to per km^2. Multivariate regressions were run on the logarithm of the two indicators as both distributions are lognormal. In this respect, an extensive database of variables potentially affecting emissions was computed at the TAZ level for the MMR. The database includes a range of socio-economic, land-use and transportation related variables (e.g. population, residential density,

[1] The same measure is used in Chapter 6, however the estimation process differs and is explained in Section 6.2.

[2] Start emission estimates were not available at the time of this study, and so NOx was chosen as the target pollutant (in contrast to Chapters 4 and 6, where HC was favoured due to its strong connection to start emissions).

highway length, etc.). The population data was estimated through data from the 2008 OD survey (AMT, 2010). Factor analysis is then employed in order to structure the large dataset into a number of factors for use in the linear regression. The individual variables were first classified into two categories: (1) variables affecting travel demand (e.g. car ownership, average income, vehicle age, etc.), and (2) variables affecting transport supply (e.g. network density, bus stop density, walkability, etc.).

The results of the factor analysis are shown in Table 3. Based on the six demand variables, three factors were derived. The first factor (i.e. high income, newer vehicles) represents the effect of household income and vehicle age. A zone that exhibits a high value for this factor can include more households with high income and newer vehicles. The second and third factors represent high vehicle ownership and larger vehicles (second factor) and older vehicles (third factor). Cumulatively, the three factors account for 81.5% of the variability in the six demand-based variables. Based on the supply variables three factors were derived to capture the effects of zones that are: (1) dense, walkable and have transit oriented development (TOD), (2) commercial, and (3) government and institutional.

Table 3 – Factor Analysis Results: Factor Loadings and Summary[a]

Demand Factors[b]	**Components**		
	High income, newer vehicles	High vehicle ownership, larger vehicles	Older vehicles
TAZ average income	0.657		
Vehicles per household		0.884	
Ratio of light-duty trucks vs. cars		0.772	
Fraction of model year: 1981 to 1990			0.949
Fraction of model year: 1991 to 2000	-0.966		
Fraction of model year: 2001 to 2011	0.956		
Summary Statistics			
Eigen Value	2.32	1.44	1.13
Variance accounted for (%)	38.62	24.03	18.89
Supply Factors[b]	**Components**		
	Dense, walkable and TOD	Commercial	Government & institutional
TAZ Walkscore	0.690		
Residential density (%)	0.732		
Length of highways (km)	-0.630		
Local road density (%)	0.862		
Open water density (%)	-0.803		
Bus stop density (%)	0.638		
Commercial area (km^2)		0.935	
Government and institutional area (km^2)			0.981
Summary Statistics			
Eigen Value	3.21	1.04	1.03
Variance accounted for (%)	40.08	13.00	12.91

[a] Principal components estimation, varimax rotation and kaiser normalization were used in creating the factors

[b] Factor loadings below 0.4 are considered insignificant and not shown in the table

5.3 Results

Spatial Distribution of Emissions

The average emitted NO_x per person (am and pm peak periods only) across the 1,552 TAZs in the region ranges from 0.0 to 17.5 grams. The spatial distribution of results across the region is shown in Figure 20. As expected, the high emitting individuals tend to reside on the periphery of the region, which is furthest from the CBD. Concurrently, the majority of low emitting individuals live centrally, on the island, much closer to the CBD. Overall, these results clearly confirm the intuitive hypothesis that high polluting individuals reside away from the downtown in suburban areas. When we overlay the map of emissions occurring on the network onto Figure 20, it is evident that most of the emissions occur in areas where the lowest polluting individuals reside (Figure 21). This is confirmed when plotting the emissions occurring within a TAZ. Indeed, it is clear that there is much higher pollution along the main highway corridors and in the areas closer to downtown. In addition, emissions are very low for all of the zones on the region's periphery. The spatial distribution of NO_x emissions per km^2 is presented in Figure 22.

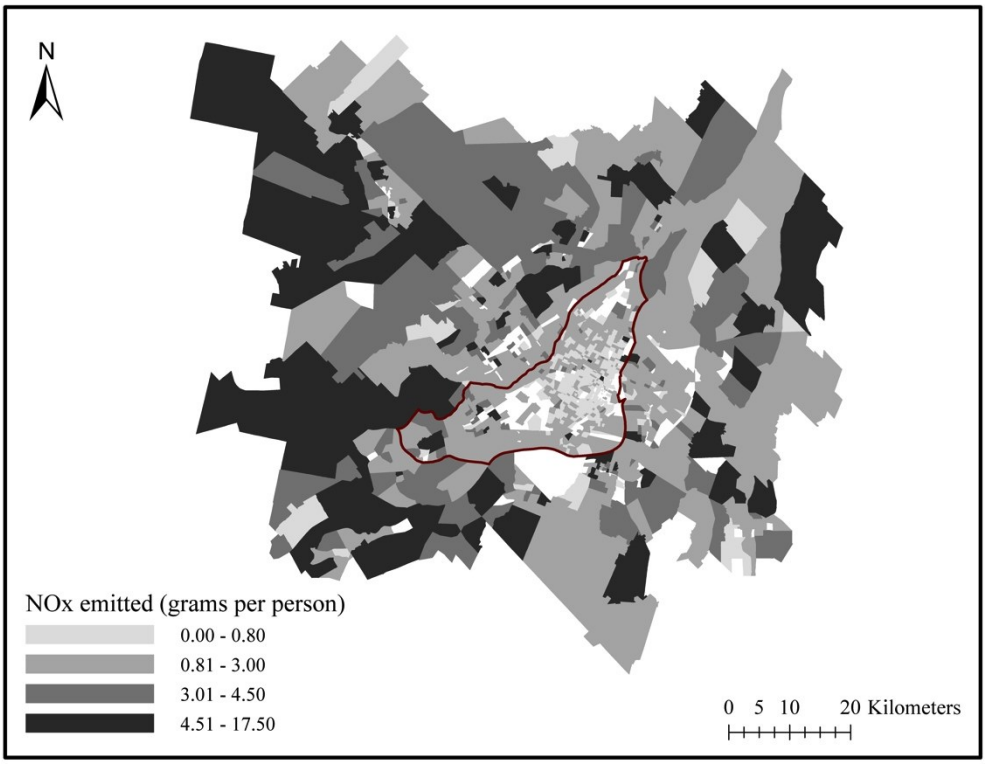

Figure 20 – Emitted NO_x per person for the MMR (island outlined in red)

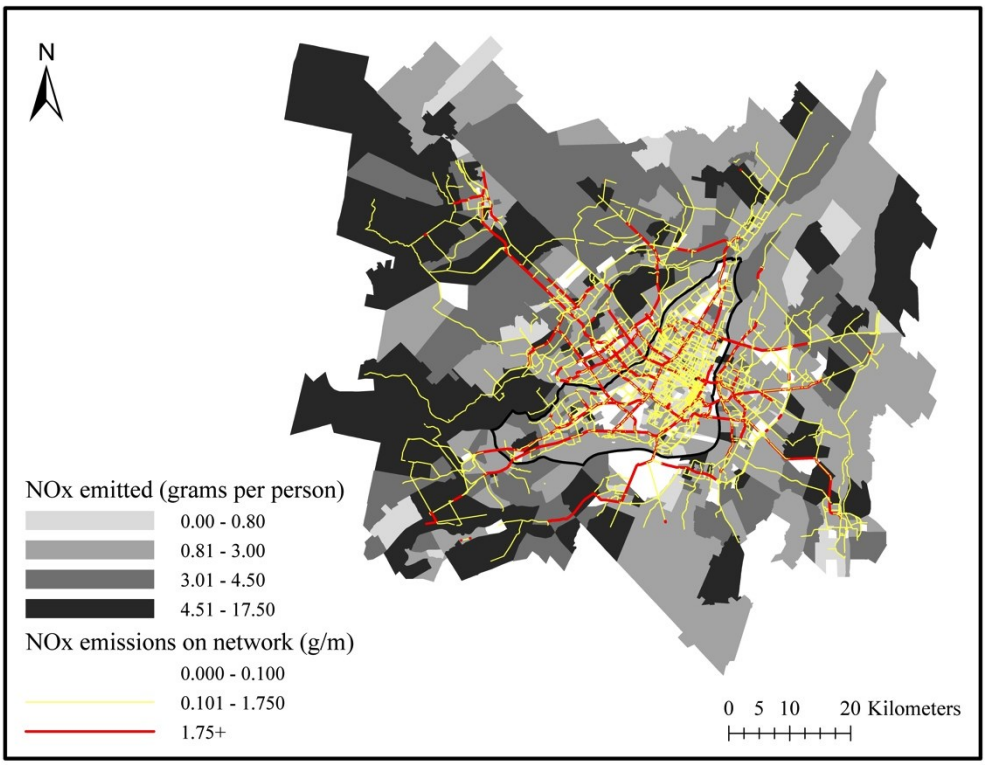

Figure 21 – Link-level NO_x emissions overlaid on a map of emitted NO_x per person

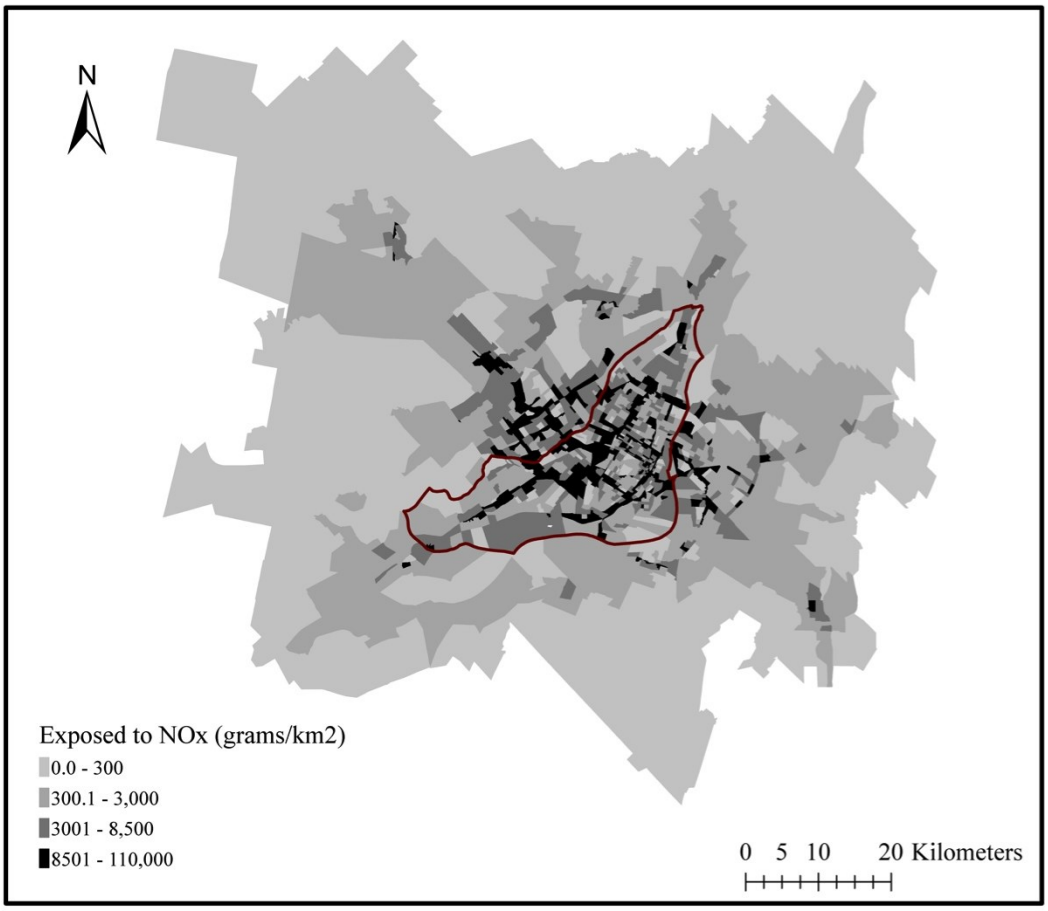

Figure 22 – Exposed to NO_x per km^2 for the MMR (island outline in red)

Statistical Analysis

In order to better understand the underlying factors associated with the generation and exposure to emissions, the two indicators of emissions were regressed against the set of factors derived from socio-economic, land-use and transport supply variables at the TAZ level. A summary of the regression results is presented in Table 4.

Table 4 – Multivariate Regression Results for ln (emitted NO_x / person) and ln (exposed to NO_x / km^2)

Factors	Ln (emitted NO_x / person)		Ln (exposed to NO_x / km^2)	
	B	**t-stat**	**B**	**t-stat**
Constant	0.077	2.543	7.103	96.02
Dense, Walkable, TOD zones	-0.082	-2.166	0.687	7.883
Government & Institutional	-0.042	-1.390	-0.120	-1.610
Commercial	-0.111	-3.497	0.238	3.147
Older Vehicles	-0.304	-9.702	-0.408	-5.507
High car ownership, larger vehicles	0.666	15.74	-0.856	-9.747
High income, newer vehicles	-0.096	-3.134	0.115	1.535
Summary Statistics				
Adjusted R^2	0.314		0.192	

We observe that the emitted NO_x per person per TAZ are positively associated with high car ownership and larger vehicles and negatively associated with dense, walkable, TOD zones. Commercial zones also tend to decrease the average individual emissions since zones with higher amounts of commercial land-use tend to be located in areas with higher accessibility, thus reducing trip length. In addition, zones with high income and newer vehicles tend to decrease individual level emissions. This is likely because newer vehicles have lower emission factors. It is important to distinguish this factor from 'high car ownership and larger vehicles'. This factor (high income, newer vehicles) seems to represent high-income urban dwellers who are not necessarily high emitters. This is an interesting finding, since it indicates that income influences emissions generation only when it is connected to higher car ownership. The final factor with negative association is 'older vehicles'. The negative sign is counter-intuitive since older vehicles tend to have significantly higher emission factors (Figure 23). This finding is however confirmed by examining the level of car ownership of owners of older vehicles. Indeed, a cross tabulation of car ownership and average vehicle age (Table 5) confirms that the factor 'older vehicles' also includes low vehicle ownership. In fact, there is clear evidence indicating that a lower vehicle

ownership leads to lower vehicle mileage (NHTS, 2009). We can then conclude that households with older vehicles tend to make fewer trips therefore offsetting the higher emissions of their vehicles.

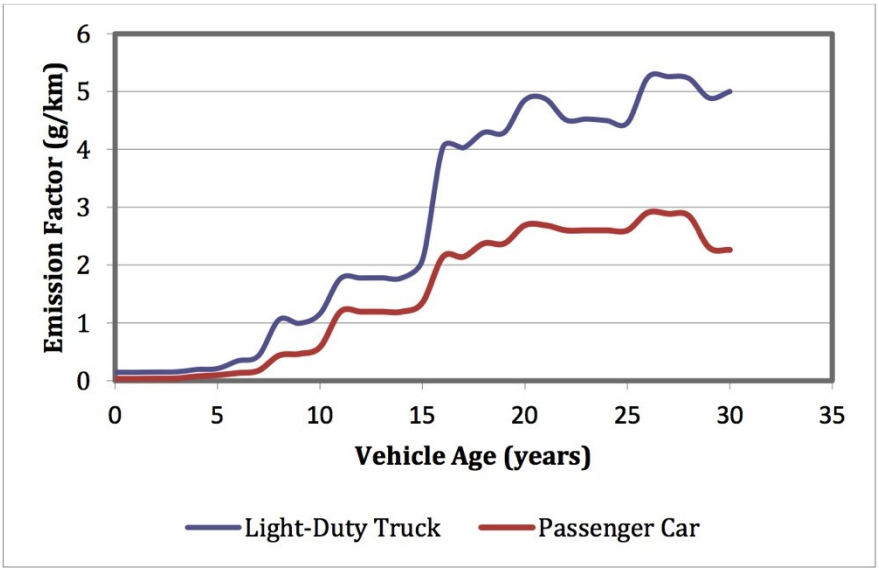

Figure 23 – Emission factor vs. vehicle age (at a constant speed of 25 mph) derived from MOVES

Table 5 – Cross-Tabulation of Vehicles per Household vs. Model Year: 1981-1990 (%)

		Vehicles per Household							
		0-0.5	0.5-1	1-1.5	1.5-2	2-2.5	2.5-3	3+	Total
Fraction of	0-0.01	2	0	0	0	0	0	0	2
model year:	0.01-0.15	32	8	22	33	3	0	0	98
1981 to 1990	0.015-0.02	55	67	114	121	20	3	1	381
	0.02-0.025	66	181	180	163	26	1	0	617
	0.025-0.03	73	78	48	41	7	0	0	247
	0.04-0.04	42	39	17	49	22	1	1	171
	0.04-0.05	18	3	4	7	3	0	0	35
	0.05+	1	0	0	0	0	0	0	1
Total		289	376	385	414	81	5	2	1552

The multivariate regression model for NO_x emissions occurring per km^2 (used as a proxy for air pollution exposure) had four significant factors. Zones that were

dense, walkable, and accessible by transit or had more commercial land-use were positively associated with air pollution exposure. Meanwhile, zones with high car ownership and larger vehicles or ones with older vehicles were negatively correlated with exposure to NO_x per km^2. This is likely because zones with higher car ownership and larger vehicles are located further away from the downtown and do not attract as much traffic.

The regression analysis points towards asymmetry in the roles of the factors influencing emissions generated and exposed to. To further explore this asymmetry, we conducted a two-step cluster analysis based on the two indicators. The cluster analysis divided the 1,552 zones into four clusters: 1) low emitter, high exposure; 2) low emitter, moderate exposure; (3) high emitter, moderate exposure; and (4) high emitter, low exposure. Based on the spatial distribution of the clusters (Figure 24), it is evident that the lowest emitting zones (highlighted in white and the lightest shade of grey) are also the ones that are exposed to the highest emissions. They are mostly located in central areas and in the CBD. In contrast, high emitting zones (dark grey) are also exposed to low amounts of pollution and located outside of the urban core. This analysis points towards spatial and socio-economic disparities in air pollution generation and exposure.

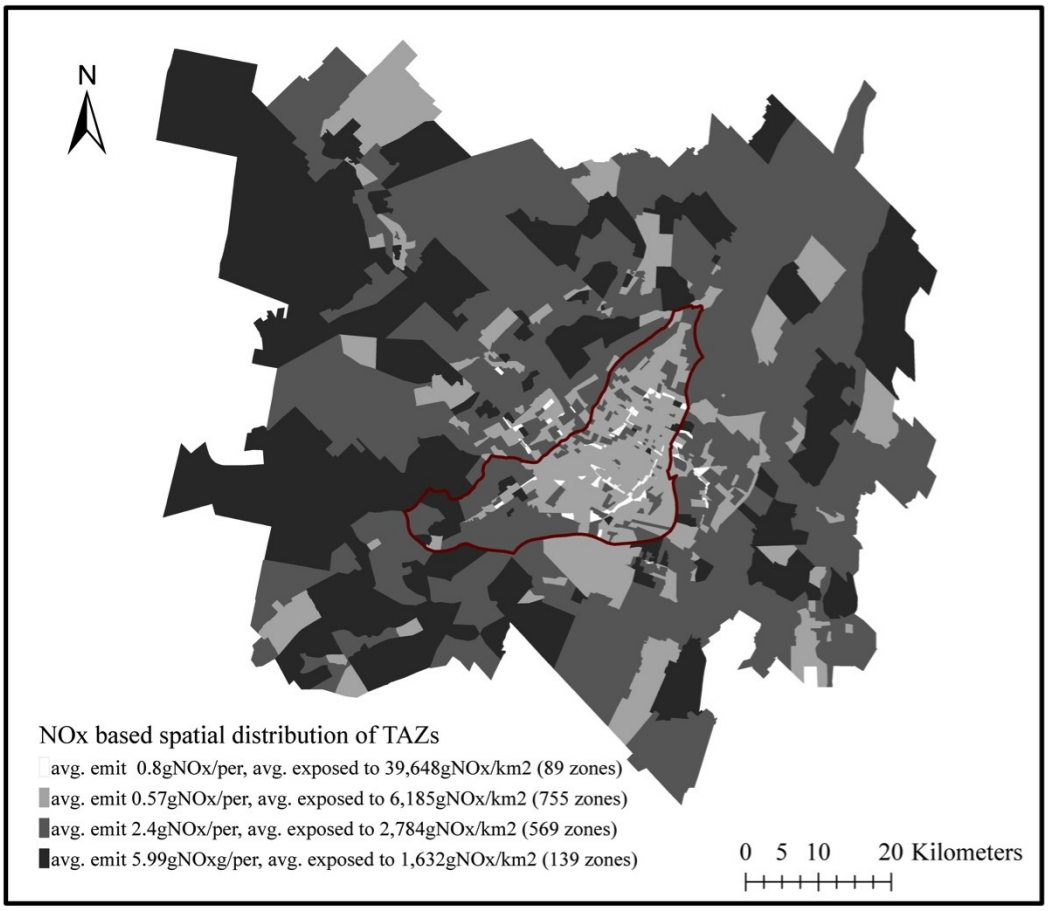

Figure 24 – Spatial distribution of the generated clusters (island outlined in red)

It is interesting to situate these results within the context of the region's spatial economy. As has been mentioned, the central areas of Montreal have a large disparity in jobs vs. residents, matched on the opposite side of the spectrum by areas such as Laval or Longueuil, which only have between 6-7 jobs for every 10 residents. It has also been shown that the CBD is the only employment centre attracting labour from across the entire region, in contrast to smaller suburban centres that tend to have local labour catchments (Shearmur and Motte, 2009). The central areas of Montreal therefore rely on the suburbs for labour. At the same time, a form of income redistribution is occurring wherein income, often high income, is made through employment in the CBD and is then transferred back to the suburbs where the high-income earners typically live (Shearmur and Motte, 2009). This income redistribution is mirrored by the results of our study which show an opposite redistribution of traffic's negative externalities from suburbs to

central areas downtown. Downtown residents are therefore faced with a net loss of wealth along with a net gain in pollution, the majority of which they are not responsible for.

5.4 Conclusions

In this chapter, we have estimated two key indicators of emissions through the development of a multi-model framework involving a regional traffic assignment model, a vehicle emissions model, and an emission post-processor. The two indicators are: (1) the average level of NO_x emissions generated per individual in a TAZ, and (2) the average level of NO_x occurring in a TAZ per km^2. Our findings indicate significant spatial disparity between the areas that generate or are responsible for high levels of individual emissions and areas that experience high emissions. Both measures were a function of socioeconomic and built environment characteristics. We observe that the factors that positively influence the emissions generated are also the ones that negatively influence the emissions occurring in a zone therefore pointing towards equity issues in the generation and distribution of traffic-related emissions.

These findings are of significant relevance to policy evaluation at the metropolitan level. When cities are faced with challenges such as reducing traffic emissions by 2030 to a certain percentage less than 1990 levels; a main question arises: Are these the emissions generated within the city or emissions generated by individuals residing in the city? In areas where residents living outside the city generate most of the traffic emissions, policy development becomes a challenging task. The modeling framework that we propose provides a way to quantify the responsibility for emissions generated and the impact of every individual's emissions on the region. It will be used to simulate regional-level transport policies and their effects on the spatial distributions of emissions and on equity in emissions generated and exposed to.

The developed modeling framework is associated with a range of limitations. In our emission modeling exercise, we focus our attention on private vehicle emissions. We are currently introducing transit emissions but we have not yet considered emissions generated by commercial traffic (freight and delivery trucks). The task of obtaining data on commercial traffic is far from trivial. In terms of traffic assignment, we employed the Stochastic User Equilibrium algorithm. We do intend to explore more advanced assignment procedures including Dynamic Traffic Assignment for generating inputs to the emission post-processor. Moreover, our current implementation of vehicle allocation is based on the vehicle type/age distribution of the residential zone of the trip-maker while not explicitly accounting for factors related to household vehicle use and potential trip chaining. In future research attempts, a vehicle allocation model based on data related to the use of specific vehicles for specific trips and by specific individuals will be developed. The nearest future extensions for this model include: linkage with dispersion models, estimation of population exposure, quantification of equity, and the evaluation of policy scenarios.

CHAPTER 6:
EQUITY IN THE GENERATION AND EXPOSURE TO TRAFFIC-RELATED AIR POLLUTION

6.1 Context

Equity in the field of transportation and land-use planning has traditionally dealt with the equal distribution of resources in the transportation system in order to support equal levels of accessibility and mobility. At the same time, there has been a parallel stream of equity research into issues of environmental justice, which tend to focus on whether marginalized or disadvantaged communities bear the brunt of pollution, be it from energy production, waste management, or transportation externalities. With the disappearance of most industry and energy production in urban areas, transportation is now the biggest contributor to urban air pollution (Colvile, et al., 2001). Traffic-related air pollution is a byproduct of the combustion process that occurs in the majority of automobiles and trucks, producing a host of pollutants such as PM, NO_x, VOCs, and more. A significant amount of research over the past 10-15 years has linked the aforementioned pollutants with a host of chronic and acute health effects (Brauer et al., 2008; Gan et al., 2012; Selander, et al., 2009). Furthermore, the spatial distribution of traffic-related air pollution is not uniform across urban metropolitan regions, resulting in exposure disparities across different population groups. Previous research has consistently shown that areas with higher levels of social disadvantage tend to have worse levels of air quality, creating a 'double-burden' of high disadvantage and high risk of air pollution related illness (Fan et al., 2012; Goodman et al., 2012; Jephcote and Chen, 2012; Crouse et al., 2009b; Jerrett, 2009).

In this chapter, we test two hypotheses related to the distributional effects of traffic-related air pollution in a large metropolitan area. First, we test the traditional hypothesis that individuals living in neighborhoods characterized by a high social disadvantage metric are also exposed to the highest levels of traffic emissions. In addition, another hypothesis is tested that neighbourhoods experiencing a certain level of traffic emissions are also responsible for similar

levels of emission generation (through travel behavior of inhabitants), often termed as the polluter-pays principle (PPP). To assess these two hypotheses, two measures of traffic-related air pollution are estimated: (1) an average level of traffic-based emissions generated per household in each TAZ and (2) an average density of experienced traffic-based emissions, also calculated at the TAZ. A cumulative index of social disadvantage is also estimated in order to highlight the most marginalized zones within the study area. Our analysis aims to investigate the relationships between the index of social disadvantage and traffic-related air pollution generation and exposure.

Traffic-related air pollution has been an important environmental justice concern since the late 1990s, and has spurred an array of studies into the linkages between exposure and socio-economic status (SES). Most of this research has focused on assessing whether inequities exist in the spatial distribution of air pollution across metropolitan regions. The two critical elements in such evaluations include (1) air pollution levels used for exposure estimates, and (2) socioeconomic indicators of disadvantage. The baseline for exposure in most studies is often established through measurement campaigns that collect ambient air pollution levels at specific points across urban areas. This method has been used in several cities across Canada, including Hamilton (Jerrett et al., 2001), Toronto (Buzzelli & Jerrett, 2007), and Montreal (Crouse et al., 2009b), as well as in London, UK (Goodman et al., 2012). At the same time, several other studies have attempted to directly estimate traffic's contribution to air pollution through the use of emission models whereby a density of traffic emissions is used as a proxy for air pollution levels without the reliance on dispersion modelling. Outputs from an emission model are then used to estimate residential exposure levels, with this method being used in studies in Christchurch, New Zealand (Kingham et al., 2007); Leicester, UK (Jephcote and Chen, 2012); Hong Kong, China (Fan et al., 2012); and Great Britain (Mitchell and Dorling, 2003). Several studies have even used proximity to high-density roads as a surrogate for exposure to traffic related air pollution (Bae et al., 2007).

Groups and neighbourhoods with lower SES have consistently been shown to experience higher levels of air pollution, a conclusion further confirmed in a summary review by Jerrett (2009). Nonetheless, Buzzelli and Jerrett (2007) found that certain centrally located, high-status zones were also susceptible to higher exposures. Crouse et al (2009b) found similar central areas where exposure levels crossed social and economic boundaries. Mitchell and Dorling (2003) also concluded that the poorest experienced the worst air quality, yet the least poor did not have the best air quality. Several of the aforementioned studies also tried to address the issue of the PPP, wherein neighbourhoods with high exposure levels contribute equally high levels of pollution thereby negating the sense of inequity. Mitchell and Dorling (2003) found that the PPP was applicable to a certain percentage of high exposure zones across Great Britain, while Jephcote and Chen (2012) found similar results for the central areas of Leicester, UK.

Regarding the socio-economic side of equity research, there has been much interest in the identification of marginalized or disadvantaged segments of the population. The history of measuring social disadvantage (often termed deprivation) has evolved over time, leading to the creation of a measure of cumulative disadvantage through combinations of a set of socio-economic measures. Cumulative disadvantage indicators tend to incorporate factors that are linked to the independent variable being studied, for instance with car ownership for transportation equity studies, or with parental education for a study on pediatric health (Bauman et al., 2006). The motivation behind the cumulative disadvantage approach is that a combination of socio-economic factors is more representative of a population's disadvantage, in that it can account for both material and social elements. Certain studies have found that social disadvantage indicators should be tailored to country-specific conditions (Sanchez-Cantalejo et al., 2008). Kingham et al (2007) employed a similar methodology in using a deprivation index that was unique to New Zealand. This line of research has also been extended to Quebec, and even Montreal. Langlois and Kitchen (1996) first proposed the use of a Montreal-specific index of General Urban Deprivation

employing the number of young residents, low-quality housing, unemployment rate, ethnicity, and youth employment participation. Pampalon and Raymond (2000) developed a similar Quebec-specific Deprivation Index that consisted of education level, employment rate, household income, marriage status, single-parent families, and number of people living alone. Meanwhile, Apparicio et al (2007) also created a Montreal-specific index of social deprivation, again accounting for the common factors of income, lone-parent families, unemployment rate, education level, and immigration. Most recently, Foth et al (2013) developed an index of social disadvantage for Toronto that combines a weighted average of median income, unemployment rate, rate of immigration within the last 5 years, and rate of households that spend over 30% of their income on rent.

In this chapter, advancements in emission modeling are used to directly estimate traffic's contribution to intra-urban air pollution. This contribution is extended to capture residential exposure levels to total HC, a common traffic-related pollutant and smog precursor, while at the same time quantifying 'responsibility' through estimating the generation of car-based HC. The two traffic-related pollution measures are then combined with a social disadvantage index to form a three-dimensional analysis involving social and environmental inequities.

6.2 Methodology

Three measures are estimated in this chapter: (1) generation of emissions per household; (2) exposure to emissions via residential zone; and (3) index of social disadvantage. The first two measures are based on outputs from the integrated transport and emission model. Specifically, the first measure regarding emission generation is the daily average emissions generated per household, calculated by normalizing total daily TAZ emissions by the number of households (kg/household).

Exposure to Traffic-Related Air Pollution

The second measure involves deriving population exposure levels to traffic-related emissions for the same set of TAZs across the Montreal region. In the absence of a dispersion model, we use the emissions occurring in the residential TAZ as a measure of population exposure. This is the same measure as was used in Chapter 5, however the estimation process differs in that it employs buffers and accounts for start emissions. Rounded buffers were created around each link to approximate dispersion effects. The buffer sizes are dependent of road type and range from 10 meters for local roads to 50 meters for expressways. The range of buffer sizes employed parallel findings from field measurements (Padro-Martinez et al., 2012) and is more conservative than typical residential buffers used in previous literature (Bae et al., 2007). Link-level running emissions generated in section 3.4 are then spatially allocated to each TAZ based on the intersecting percentage of the road buffer. At the same time, vehicle start emissions are assumed to occur entirely in the origin TAZ of each trip. Average exposure values are then calculated by normalizing the total HC emitted by the land-area of the TAZ to generate an average emission density (kg/km^2).

Social Disadvantage Index

The estimation of a social disadvantage index (SDI) follows a similar methodology to the one used in Foth et al (2013), although there is a difference in spatial resolution. The SDI is estimated at the TAZ level instead of the census tract (CT) level in order to maintain consistency with the measures for traffic-related emissions. At the same time, TAZs are at an even finer level of detail than CTs, which are often delineated in order to capture relatively homogeneous socio-economic neighborhoods. The improvement in resolution should serve to provide clearer associations with exposure to traffic emissions, as has been previously found in Goodman et al (2011). The following socio-economic data from the 2006 census were retrieved at the CT and census subdivision level (Statistics Canada, 2006):

- Median household income
- Unemployment rate (percentage of labor force that is unemployed)
- Percentage of population that had immigrated within the last 5 years (2001-2006)
- Percentage of households that spend over 30% of their income on rent

Despite the fact that no correlation was found between immigration status and disadvantage in previous studies (Crouse et al., 2009b), immigration rate was still included in order to ensure that the elements of social disadvantage (unemployment and immigration) were equally as present as elements of material disadvantage (income and % of income spent on rent).

After the four variables were retrieved for all CTs and census subdivisions in the region, the amount of habitable land was estimated for each TAZ based on land-use information for the region (all land-uses aside from 'open water' and 'parks and recreation' were considered 'habitable'; DMTI, 2007). The area of habitable land was then used to create area-based weights, and subsequently population-based weights, that were used in converting the four variables from CT to TAZ level. Each variable was then standardized and weighted equally to create the SDI (see equation 1).

$$SDI = Z_{Unemployment\ Rate} + Z_{Immigration\ Rate} + Z_{30\%\ of\ Income\ on\ Rent} - Z_{Median\ Income} \quad (1)$$

For instance, a zone with a median household income of $48,758 (Z-score = -0.196), unemployment rate of 7.8% (Z-score = 0.246), recent immigration rate of 11.4% (Z-score = 1.567), and having 32.6% of households that spend over 30 percent of income on rent (Z-score = 1.388), has an SDI of 3.397. A correlation matrix was calculated to ensure that the index is capturing similar socio-economic groups, and the four variables were all significantly correlated with Pearson coefficients above 0.44 (significant at the 0.01 level). The SDI results were then

normalized into deciles and each TAZ was given a score between 1-10 based on its respective decile. There were zones with either no reported population or insignificant data available and so TAZs with populations below 1 were omitted from the analysis, resulting in a sample size of 1513 TAZs.

Statistical Analysis

An empirical analysis was conducted to examine the relationships between the estimated SDI and the two measures of traffic emissions (emissions generated per household and emissions occurring in a TAZ); both measures accounting for running and start emissions. Analyses were conducted using data normalized in deciles, as has been favoured in several equity studies previously conducted (Fan et al., 2012; Mitchell & Dorling, 2003).

Social disadvantage and exposure

The first measure is calculated by taking the difference between the social disadvantage decile and the exposure decile. This measure ranges from -9 to 9, and serves to test the relationship between disadvantage and exposure. For instance, if there are many values clustered around zero then there is likely a positive relationship between disadvantage and exposure (ie. zones with high disadvantage have high exposure, and zones with low disadvantage have low exposure). Otherwise, a high positive value means that the zone has high disadvantage and low exposure, and a high negative value means low disadvantage and high exposure. In addition to that, the sum of SDI and exposure deciles is taken in order to spatially highlight zones that face a 'double-burden' of greater disadvantage and higher amounts of air pollution.

Exposure and emission generation

Another measure is calculated that aims to capture whether the responsibility in emission generation is being matched with equivalent exposure to air pollution. This 'polluter-pays index' is calculated by taking the difference in the exposure decile and the emissions decile, with values ranging from -9 to 9. Inequity is

therefore evident if there are many zones in the lowest or highest areas of that range, for instance if there are many neighbourhoods that have high exposure and low emission responsibility or vise versa. Otherwise, if a majority of zones are relatively close to zero, then the polluter-pays principle likely applies.

Social disadvantage, exposure and emissions

The final measure involves adding the third dimension of emission generation to the previously explored concept of disadvantage combined with air pollution exposure. The measure is calculated by taking the sum of the SDI decile and the 'polluter-pays index' [SDI + (Exposure – Emissions)]. Only the uppermost and lowermost values are of interest in this analysis. The uppermost values correspond with zones that are highly disadvantaged, have high exposure to air pollution and generate low amounts of emissions. Meanwhile, the lowermost values are those with low disadvantage, low exposure and who generate the highest amounts of traffic-related air pollution.

6.3 Results

The distribution of raw values for the social disadvantage index is slightly skewed to the right, and range from – 13.64 to 13.54 (Figure 25). Table 6 illustrates the SDI values divided into deciles; we observe large discrepancies in the four socioeconomic factors between the lowest SDI values (1st decile) and the highest (10th decile). The spatial distribution of the SDI deciles across the MMR can be seen in Figure 26. The areas of highest social disadvantage are distributed across the island of Montreal with the highest concentration around the denser inner parts of the city. Other socially disadvantaged neighborhoods (8-9th deciles) are also heavily concentrated in central areas on the island, including large portions of the boroughs of Ahuntsic-Cartierville, Côte-des-Neiges, Hochelega-Maisonneuve, Le Sud-Ouest, Parc-Extension, and Ville-Marie. At the same time, the wealthy enclaves of Westmount, Outremont, and Mont-Royal are all visibly present near downtown, as well as the suburban neighbourhoods in the west part of the island. The spatial SDI results for the island of Montreal parallel similar findings in

previous research (Crouse et al., 2009b; Apparicio et al., 2007; Langlois and Kitchen, 1996). Aside from Montreal, most of the region is almost entirely under the 50th percentile for social disadvantage, aside from pockets in the cities of Laval and Longueuil.

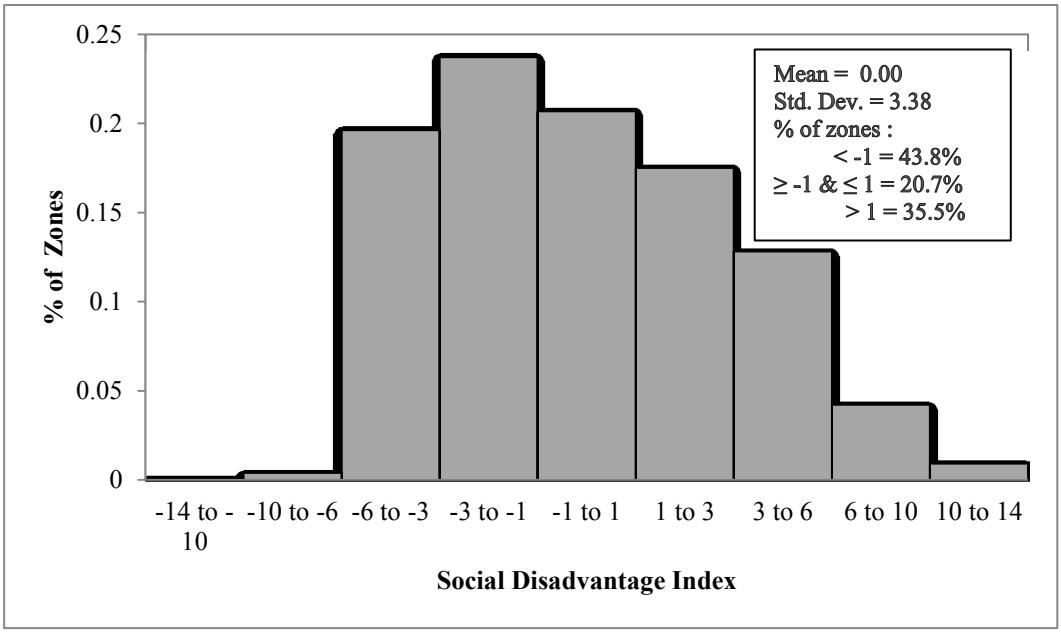

Figure 25 – Histogram of the raw values of the Social Disadvantage Index

Table 6 – Comparison of Socioeconomic Variables Between SDI Deciles (mean values)

Socioeconomic Variable	1st decile	Mean	10th decile
i) Median Household Income (CAD)	91,319	52,856	29,759
ii) Unemployment Rate (%)	3.5	6.9	13.8
iii) Immigration Rate (2001-2006; %)	1.3	4.3	13.9
iv) Households that spend over 30% income on Rent (%)	3.0	16.3	35.8

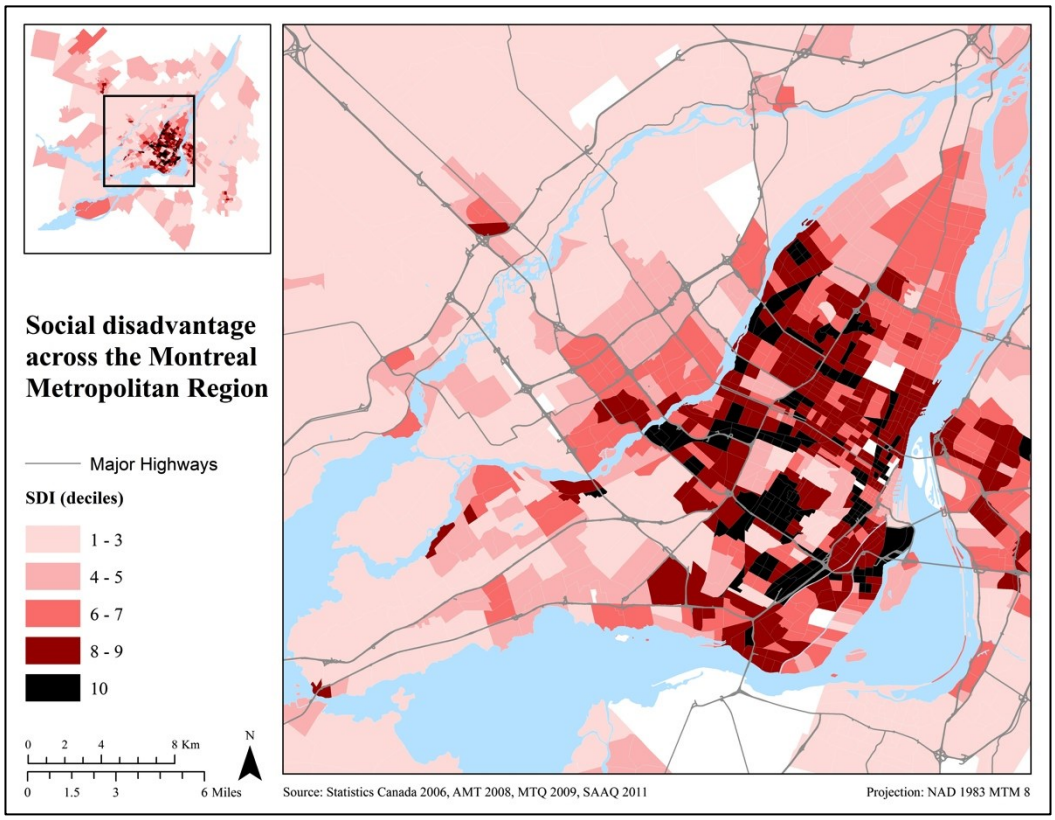

Figure 26 – Social Disadvantage Index deciles across the MMR

Further examination of Figure 26 reveals that many of the most socially disadvantaged neighborhoods are located in close proximity to major highways that typically carry high traffic flows. Meanwhile, the majority of wealthier neighborhoods appear to be in areas that are relatively free of major highways. This initial observation suggests the existence of a socio-economic gradient in traffic-related air pollution exposure. This relationship is further explored by observing the difference in decile rankings between SDI and exposure (Figure 27). We observe that 50% of zones have comparable rankings in SDI and exposure; the difference between their SDI and exposure is between -1 and +1. This indicates that a positive correlation between SDI and exposure exists; higher disadvantaged neighbourhoods tend to have higher exposure levels and vice versa. The other 50% of zones are split almost equally between areas with 'high social disadvantage and low exposure' (difference is greater than 1) and areas with 'low social disadvantage and high exposure' (difference is less than -1).

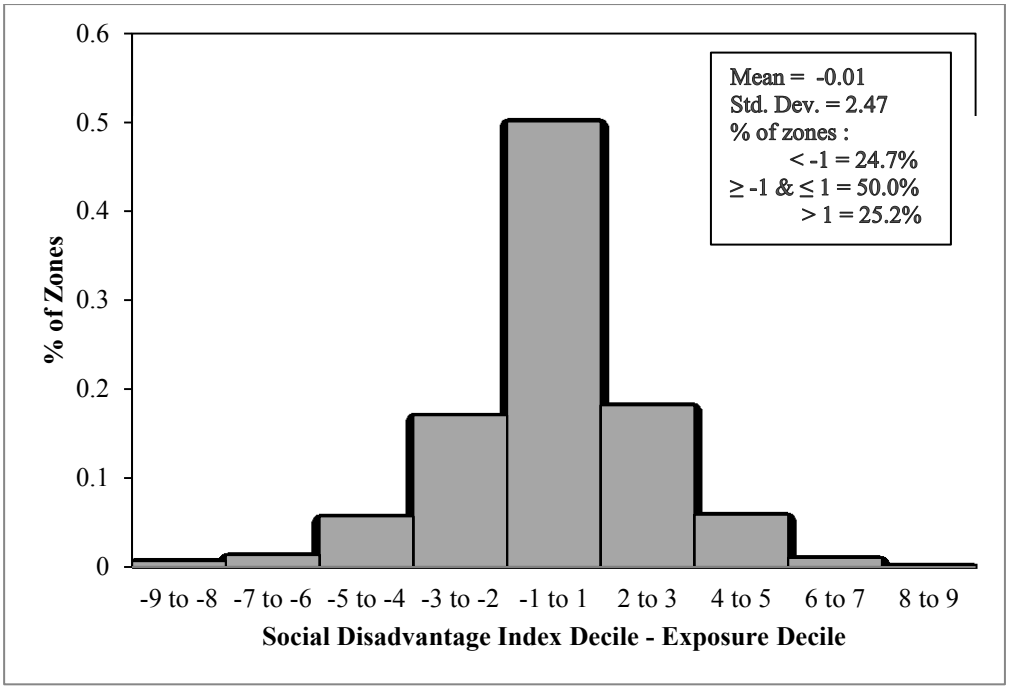

Figure 27 – Histogram of the difference in rankings between SDI and exposure

The second measure of social disadvantage and population exposure is calculated involving the summation of SDI and exposure decile rankings. The spatial distribution of the resulting measure can be seen in Figure 28. Neighbourhoods with combined SDI and exposure greater than 18 were of most interest, as these are the neighborhoods that experience the 'double-burden' of greatest disadvantage and highest traffic-related air pollution exposure. The majority of these neighbourhoods border the major highways that surround the central part of the island of Montreal. Neighbourhoods within the Plateau Mont-Royal and Rosemont boroughs also experience a similar double-burden through their proximity to high traffic densities on arterial roads. At the same time, certain neighbourhoods facing a double-burden exist outside of the central areas, as there are pockets of 'high disadvantage and high exposure' in the borough of Montréal Nord, northeast of Saint-Léonard, and in Longueuil.

The majority of the region outside of Montreal falls into the bracket of lowest disadvantage and exposure. However, it is interesting to note that there are several

neighborhoods close to downtown, specifically Westmount, Outremont, and parts of Mont-Royal, that are categorized in the same bracket. This finding contradicts those in Crouse et al (2009b), which found that the very same central neighborhoods in Montreal with higher SES also experienced relatively higher air pollution. This discrepancy in findings is likely because the buffer sizes used in linking road emissions to TAZs were more conservative than other methods for generating spatially refined air quality levels.

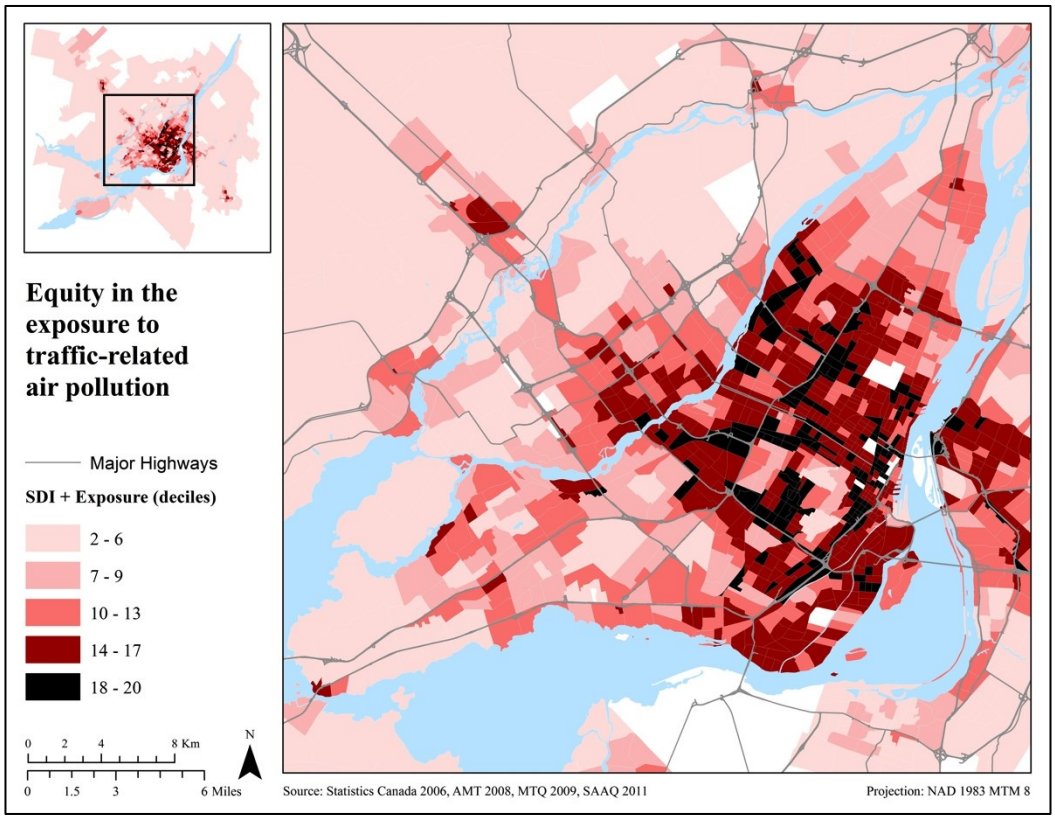

Figure 28 – Sum of social disadvantage ranking and exposure ranking across the MMR

Aside from direct exposure inequity, it is also interesting to test whether the PPP is in effect across the Montreal region. In order to test for PPP, a polluter-pays index that takes the difference between exposure ranking and emission ranking was calculated, and the resulting histogram is shown in Figure 29. Given that only 22.2% of zones have equivalent exposure and emission rankings, it seems as if the polluter-pays principle is not generally applicable to the region. At the same time,

nearly 40% of neighborhoods 'pay' more than they contribute in terms of traffic-related air pollution, while 38% are contributing more than they 'pay'.

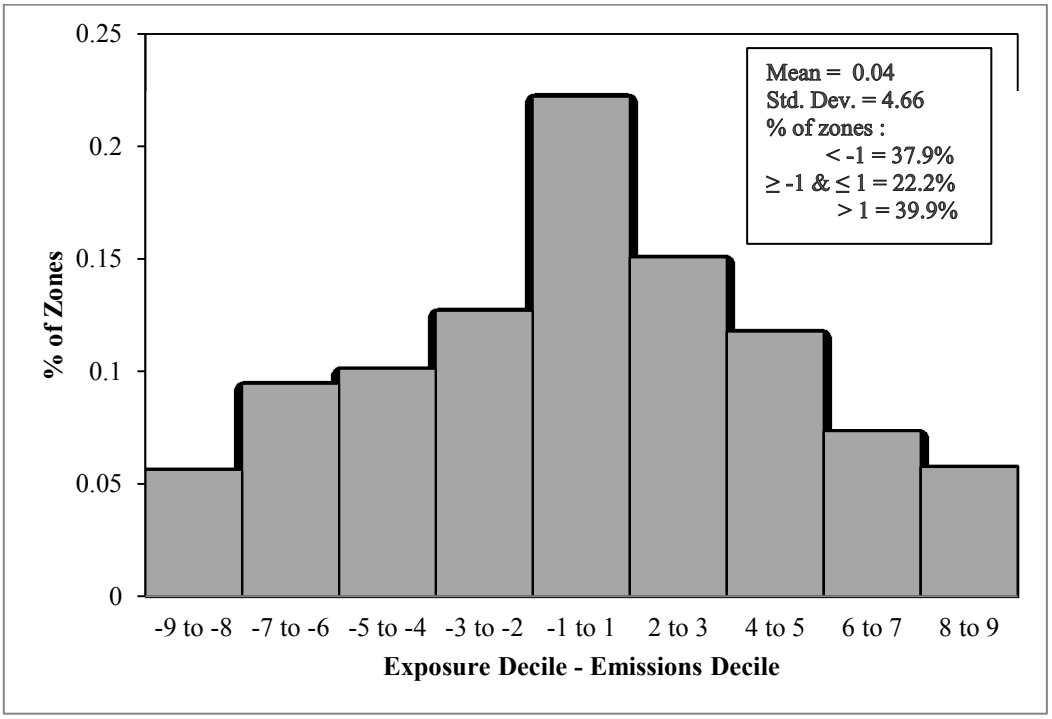

Figure 29 – Histogram of the difference in rankings between exposure and emission generation

The polluter-pays index was mapped in order to observe whether the inequity has a spatial component as well, or whether the neighbourhoods exhibiting PPP are geographically linked (Figure 30). The spatial distribution across the MMR is variable yet much of the central areas near downtown and along highway corridors have higher rankings in exposure over emissions. There are also neighbourhoods in the CBD and along the most heavily trafficked freeways with extreme gradients between exposure and emission generation (differences of 8 or 9 deciles). Neighbourhoods exhibiting PPP with a polluter-pay index between -1 and 1 are scattered across Montreal, Laval and Longueuil, with no real spatial pattern. Meanwhile, peripheral areas of the region are almost entirely on the negative side of the distribution with differences in exposure vs. emissions ranging from -2 to -9, a finding consistent with a similar study conducted in the UK (Jephcote and

Chen, 2012). Therefore, not only is the polluter-pays principle absent for most of the MMR, the inequity is also spatially biased towards central neighborhoods closer to Montreal's downtown. While this finding is important, it is not altogether surprising given that central neighbourhoods have some of the highest traffic levels while at the same time having residents who make nearly half their trips by public transit or active transportation (AMT, 2010). On the other hand, the peripheral areas of the region are much more car-reliant yet reside in neighbourhoods with light traffic volumes.

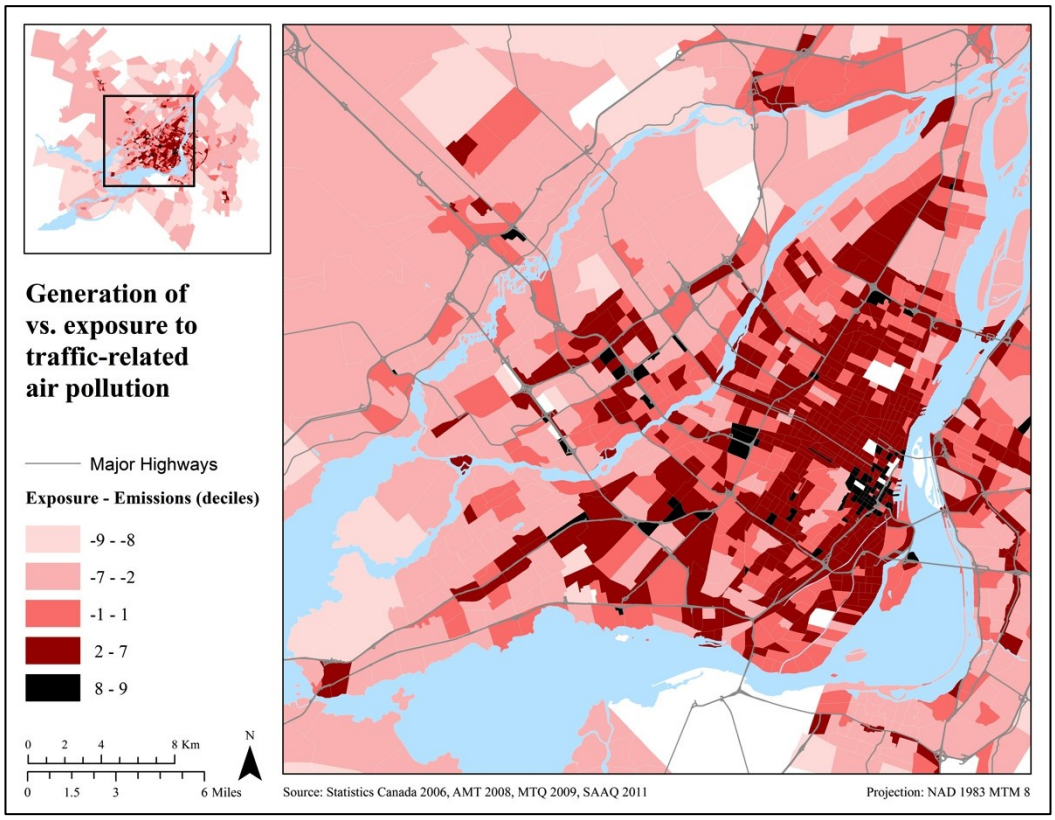

Figure 30 – Ranking comparison between emission generation and exposure

Finally, the last measure incorporating generation/exposure ranking and SDI was calculated in order to add another dimension in combining the ideas of 'polluter pays' with socioeconomic equity. The resulting spatial distribution is shown in Figure 31, and confirms that there are numerous neighborhoods, primarily in the central areas closer to downtown (shown in black), that have the 'double-burden'

of social disadvantage, higher traffic-related air pollution *and* contribute very little of the pollution they are experiencing. This finding contradicts several conclusions made by both Mitchell and Dorling (2003) and Jephcote and Chen (2012) who found that centrally located disadvantaged neighborhoods actually produced comparable levels of traffic-related air pollution to those they were experiencing. The difference in findings could be due to methodological differences, although it could again be attributed to the high levels of transit use and lower car-based travel distances amongst these central Montreal neighborhoods (AMT, 2010). Again, the peripheral areas of the region are almost unanimously of low disadvantage, with low exposure to traffic-related air pollution, while at the same time often generating the highest amounts of emissions.

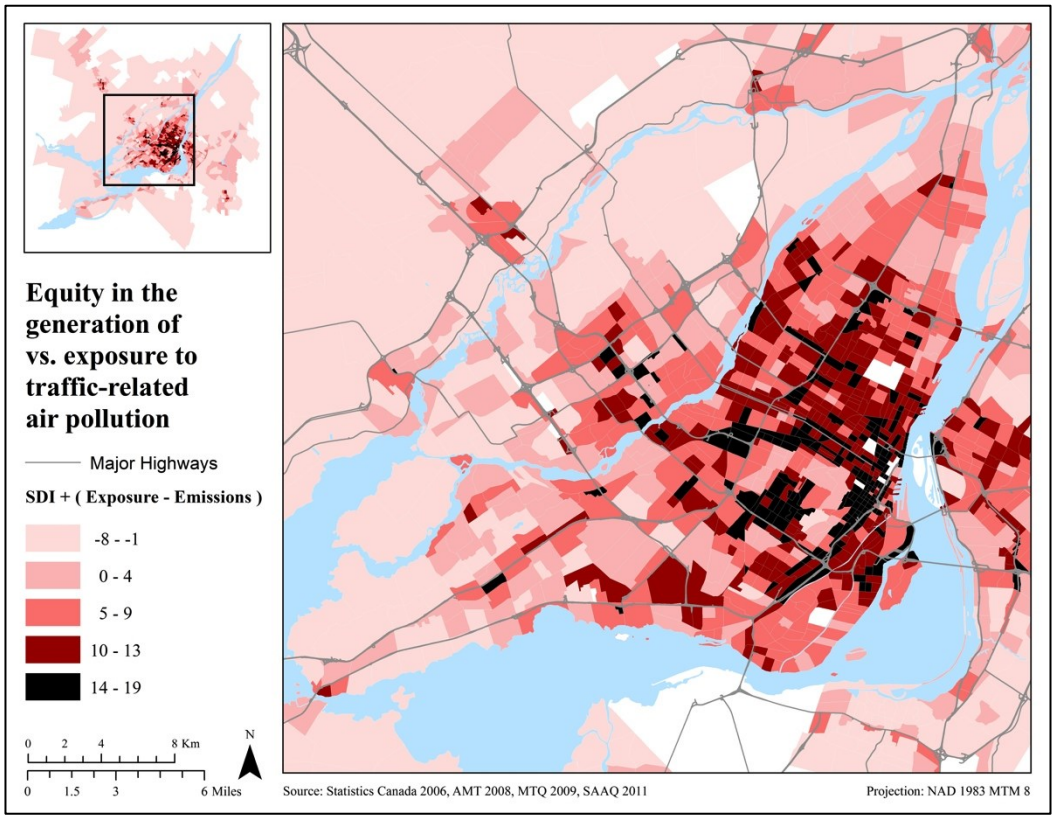

Figure 31 – Socioeconomic equity of traffic-related air pollution generation and exposure

6.4 Conclusions

This chapter has explored the relationships between traffic-related air pollution generation, exposure, and socioeconomic disadvantage. Two measures of traffic-related air pollution are estimated; one that captures the generation of HC emissions per household, and another that captures location-based exposure to HC emissions. In addition, an index of social disadvantage was developed that incorporates elements of both social and material deprivation. The findings from this study suggest three levels of environmental injustice occurring across the Montreal region. The first is that neighborhoods with the highest social disadvantage experience the worst exposures to traffic-related air pollution, confirming similar findings across cities in North America and beyond. At the same time, the polluter-pays principle is mostly absent given that the majority of neighborhoods in central areas experience much higher levels of air pollution than they are responsible for. In addition, there is a subset of those same central neighborhoods that are highly disadvantaged communities who are being exposed to higher levels of pollution that they have little to no role in producing. Given the findings of social and environmental inequities, it would be interesting to extend the analysis to testing whether a 'triple-jeopardy' situation exists that includes an additional dimension of health inequities.

There were a few limitations with this analysis. Commercial truck traffic was not factored into the exposure measure. This omission could result in an under-prediction of pollution levels in the socially disadvantaged areas, given the previous associations seen between lower-income areas and heavy-duty truck traffic (Houston, et al., 2008). The index of social disadvantage employed in this study does not capture elements that might show increased susceptibility to air pollution exposure such as higher presence of young children, elderly people, people with previous health issues, and even indigenous populations. Furthermore, the measure of exposure does not employ dispersion models to account for local variations in built environment or climactic conditions, nor does it account for a wholly detailed source-receptor relationship, as described in Beckx et al (2009b).

Despite these limitations, this research highlights three levels of inequity regarding socioeconomics and traffic-related air pollution in the Montreal region. An unfair burden of negative externalities from transport is being placed on the region's disadvantaged populations, many of whom emit some of the lowest levels of emissions. It falls to policy-makers to address these imbalances, either by targeting the highest emitters or by creating buffers for those facing the double-burden of social disadvantage and higher air pollution.

CHAPTER 7:
CONCLUSIONS AND FUTURE PATHWAYS OF RESEARCH

An integrated transport and emission model has been developed for the MMR that incorporates an average-speed regional traffic model with a comprehensive emission processor. Detailed travel behaviour information, vehicle registry data, and local environmental conditions are all accounted for in the model. Both running and start emissions are estimated at the individual and link-level with a temporal resolution of one hour. The integrated model captures the emissions of both global pollutants, such as $CO_{2\text{-eq}}$, and local pollutants, such as HC, NO_x, and CO. Link-level emissions are further extended using buffers to act as a surrogate measure of exposure to traffic-related air pollution.

The outputs from the integrated model were first used to test the accuracy of emission inventories, specifically the sensitivity to variability in input data. Start emissions were found to have the greatest impact on estimates, followed by accurate vehicle registry data. Building upon those accurate estimates, the research moved forward to testing whether various land-use and socioeconomic characteristics were determinants of either traffic-related air pollution generation or exposure. Neighbourhoods with greater car ownership and larger vehicles were found have higher emission rates per household, whereas areas with higher network densities and better transit access had much higher exposure levels. In addition, large spatial disparities in both generation and exposure were observed between suburban areas and neighbourhoods closer to downtown. These disparities were then explored further in conjunction with socioeconomic standing. Three levels of inequity were observed in the MMR: (1) neighbourhoods with higher social disadvantage tend to experience higher air pollution levels, (2) neighbourhoods closer to downtown tend to experience greater levels of air pollution than they create, and (3) neighbourhoods with the greatest disparities in exposure versus generation often tend to be those with the highest social disadvantage.

While several limitations of the integrated modeling framework have been identified in previous chapters, it is worth highlighting them again especially in light of future pathways for research. The first major exclusions from the integrated model are public transit and commercial heavy-duty freight traffic, both large components under the umbrella of road transport. Public transit is likely easier to include in the analysis given that data are much more available than information from private freight companies. Another model limitation is that the current integrated framework does not include dispersion effects after the link-level emissions are estimated.

Despite these limitations, the future for integrated transport and emission models is bright. With the current state of computing, the models can be extended to entire metropolitan regions and even certain countries, depending on size. Integrated models are invaluable tools for planners in estimating accurate road transport emission inventories, measuring intra-urban variations in residential exposure levels, assessing metropolitan-wide levels of responsibility for emission generation, and more. In addition, they are crucial for assessing the effectiveness of future policy scenarios regarding emission reduction targets or regional air quality management strategies.

Therefore, future pathways of research include incorporating public transit and freight traffic into the integrated framework as well as adding a dispersion model. At the same time, the regional traffic assignment model can be updated to one that is based on activities and agents rather than trips and flows. The combination of an activity- and agent-based model in conjunction with dispersion modeling would provide highly detailed source-receptor relationships for use in exposure studies. Overall, the addition of all previously mentioned elements would significantly strengthen the capabilities of the integrated framework in assessing future scenarios and policy implications.

REFERENCES

Agence Metropolitaine de Transport (AMT) (2010). La mobilite des personnes dans la region de Montreal: Faits Saillants. *Enquete Origine-Destination 2008.*

Anderson, W.P., Kanaroglou, P.S., Miller, E.J., and Buliung, R.N. (1996). Simulated automobile emissions in an integrated urban model. *Transportation Research Record, 1520,* 71-80.

Apparicio, P., Cloutier, M-S. and Shearmur, R. (2007). The case of Montreal's missing food deserts: evaluation of accessibility to food supermarkets. *International Journal of Health Geographics, 6 (4).*

Babisch, W., Beule, B., Schust, M., Kerbett, N., & Ising, H. (2005). Traffic Noise and Risk of Myocardial Infarction. *Epidemiology, 16 (1),* 33-40.

Bae, C-H., Sandlin, G., Bassok, A., and Kim, S. (2007). The exposure of disadvantaged populations in freeway air-pollution sheds: a case study of the Seattle and Portland regions. *Environment and Planning B: Planning and Design, 34,* 154-170.

Barla, P., Miranda-Moreno, L.F., and Lee-Gosselin, M. (2011). Urban travel CO2 emissions and land use: A case study for Quebec City. *Transportation Research Part D, 16*, 423-428.

Bauman, L.J., Silver, E.J, and Stein, R.E.K. (2006). Cumulative social disadvantage and child health. *Pediatrics, 117 (4),* 1321-1328.

Beckerman, B., Jerrett, M., Brook, J. R., Verma, D. K., Arain, M. A., and Finkelstein, M. (2008). Correlation of nitrogen dioxide with other traffic pollutants near a major expressway. *Atmospheric Environment*, *42*, 275–290.

Beckx, C., Int Panis, L., Vankerkom, J., Janssens, D., Wets, G., and Arentze, T. (2009a). An integrated activity-based modeling framework to assess vehicle emissions: approach and application. *Environment and Planning B: Planning and Design, 36,* 1086-1102.

Beckx, C., Int Panis, L, Uljee, I., Arentze, T., Janssens, D., and Wets, G. (2009b). Disaggregation of nation-wide dynamic population exposure estimates in

the Netherlands: applications of activity-based transport models. *Atmospheric Environment, 43 (34),* 5454-5462.

Bellasio, R., Bianconi, R., Corda, G., and Cucca, P. (2007). Emission inventory for the road transport sector in Sardinia (Italy). *Atmospheric Environment, 41,* 677-691.

Borge, R., de Miguel, I., de la Paz, D., Lumbreras, J., Perez, J., and Rodriguez, E. (2012). Comparison of road traffic emission models in Madrid (Spain). *Atmospheric Environment, 62,* 461-471.

Borrego, C., Tchepel, O., Salmim, L., Amorim, J. H., Costa, A. M., and Janko, J. (2004). Integrated modeling of road traffic emissions: application to Lisbon air quality management. *Cybernetics and Systems: An International Journal, 35,* 535-548.

Brand, C., and Preston, J.M. (2010). '60-20 emission' - The unequal distribution of greenhouse gas emissions from personal, non-business travel in the UK. *Transport Policy, 17*, 9-19.

Brauer, M., Lencar, C., Tamburic, L., Koehoorn, M., Demers, P., and Karr, C. (2008). A cohort study of traffic-related air pollution impacts on birth outcomes. *Environmental Health Perspectives, 116 (5),* 680-686.

British Columbia Ministry of Environment (BC MoE). (2013). Metro-Vancouver Regional District. *2010 Community Energy and Emissions Inventory*.

Buzzelli, M., and Jerrett, M. (2007). Geographies of susceptibility and exposure in the city: environmental inequity of traffic-related air pollution in Toronto. *Canadian Journal of Regional Science, XXX (2),* 195-210.

Colvile, R.N., Hutchinson, E.J., Mindell, J.S., and Warren, R.F. (2001). The transport sector as a source of air pollution. *Atmospheric Environment, 35 (9),* 1537-1565.

Corvalan, R.M., Osses, M., and Urrutia, C.M. (2002). Hot emission model for mobile sources: application to the metropolitan region of the City of Santiago, Chile. *Journal of Air & Waste Management Association, 52,* 167-174.

Chen, H., Goldberg, M. S., & Villeneuve, P. J. (2008). A systematic review of the relation between long-term exposure to ambient air pollution and chronic diseases. *Reviews on Environmental Health, 23 (4),* 243-297.

Crouse, D.L., Goldberg, M.S., and Ross, N.A. (2009a). A prediction-based approach to modelling temporal and spatial variability of traffic-related air pollution in Montreal, Canada. *Atmospheric Environment*, *43 (32),* 5075-5084.

Crouse, D., Ross, N., and Goldberg, M. (2009b). Double burden of deprivation and high concentrations of ambient air pollution at the neighbourhood scale in Montreal, Canada. *Social Science & Medicine, 69,* 971-981.

De Ridder, K., Lefebre, F., Adriaensen, S., Arnold, U., Beckroege, W., Bronner, C., et al. (2008). Simulating the impact of urban sprawl on air quality and population exposure in the German Ruhr area. Part I: reproducing the base state. *Atmospheric Environment, 42,* 7059-7069.

DMTI Spatial Inc. (2007). General land use for the Montreal region. Accessed from the Transportation Research at McGill (TRAM) GIS database on June 20th, 2013.

Environment Canada. (2011). "Distribution of greenhouse gas emissions by economic sector, Canada, 2011" Table, http://www.ec.gc.ca/indicateurs-indicators/default.asp?n=BFB1B398 accessed on July 30th, 2013.

Fan, X., Lam, K-C., and Yu, Q. (2012). Differential exposure of the urban population to vehicular air pollution in Hong Kong. *Science of the Total Environment 426,* 211-219.

Favez, J.-Y., Weilenmann, M., and Stilli, J. (2009). Cold start emissions as a function of engine stop time: evolution over the last 10 years. *Atmospheric Environment, 43,* 996-1007.

Foth, N., Manaugh, K., and El-Geneidy, A.M. (2013). Towards equitable transit: examining transit accessibility and social need in Toronto, Canada, 1996-2006. *Journal of Transport Geography, 29,* 1-10.

Frank, L.D., Sallis, J.F., Conway, T.L., Chapman, J.E., Saelens, B.E., and Bachman, W. (2006). Many pathways from land use to health: associations

between neighbourhood walkability and active transportation, body mass index, and air quality. *Journal of the American Planning Association, 72 (1),* 75-87.

Frank, L.D., Stone Jr., B., and Bachman, W. (2000). Linking land use with household vehicle emissions in the central puget sound: methodological framework and findings. *Transportation Research Part D, 5 (3),* 173-196.

Gan, W.Q., Davies, H.W., Koehoorn, M., and Brauer, M. (2012). Association of long-term exposure to community noise and traffic-related air pollution with coronary heart disease mortality. *American Journal of Epidemiology, 175 (9),* 898-906.

Goodman, A., Wilkinson, P., Stafford, M., and Tonne, C. (2011). Characterising socio-economic inequalities in exposure to air pollution: a comparison of socio-economic markers and scales of measurement. *Health & Place, 17,* 767-774.

Hao, J., He, D., Wu, Y., Fu, L, and He, K. (2000). A study of the emission and concentration distribution of vehicular pollutants in the urban area of Beijing. *Atmospheric Environment, 34,* 453-465.

Hao, J.Y., Hatzopoulou, M., and Miller, E.J. (2010). Integrating an Activity-Based Travel Demand Model with Dynamic Traffic Assignment and Emission Models. *Transportation Research Record: Journal of the Transportation Research Board , 2176*, 1-13.

Hoek, G., Brunekreef, B., Goldbohm, S., Fischer, P., and van den Brandt, P. (2002). Association between mortality and indicators of traffic-related air pollution in the Netherlands: a cohort study. *The Lancet, 360 (9341)*, 1203-1209.

Houk, J. (2004). Making use of MOBILE6's capabilities for modeling start emissions. *Proceedings of the A and WMA's 97th Annual Conference and Exhibition,* (1884), 5115-5130.

Houston, D., Krudysz, M., and Winer, A. (2008). Diesel truck traffic in low-income and minority communities adjacent to ports: environmental justice

implications of near-roadway land use conflicts. *Transportation Research Record: Journal of the Transportation Research Board, 2067,* 38-46.

ICF International. (2007). Greenhouse gases and air pollutants in the City of Toronto: Toward a harmonized strategy for reducing emissions. Prepared for: the City of Toronto. In collaboration with: the Toronto Atmospheric Fund and the Toronto Environment Office.

Intergovernmental Panel on Climate Change (IPCC). (2007). Contribution of working groups I, II and III to the fourth assessment. *Report of the Intergovernmental Panel on Climate Change.*

International Energy Agency (IEA). (2012). CO_2 emissions from fuel consumption: highlights. Prepared for: *18th Session of the Conference of the Parties to the Climate Change Convention (COP 18).*

Jephcote, C., and Chen, H. (2012). Environmental injustices of children's exposure to air pollution from road-transport within the model British multicultural city of Leicester: 2000-2009. *Science of the Total Environment, 414,* 140-151.

Jerrett, M. (2009). Global geographies of injustice in traffic-related air pollution exposure. *Epidemiology, 20 (2),* 231-233.

Jerrett, M., Burnett, R.T., Kanaroglou, P., Eyles, J., Finkelstein, N., Giovis, C., et al. (2001). A GIS-environmental justice analysis of particulate air pollution in Hamilton, Canada. *Environment and Planning A, 33*, 955-973.

Kahn, M.E. (1998). A household level environmental Kuznets curve. *Economics Letters*, 269-273.

Karppinen, A., Kukkonen, J., Elolahde, T., Konttinen, M., Koskentalo, T., and Rantakrans, E. (2000). A modelling system for predicting urban air pollution: model description and applications for the Helsinki metropolitan area. *Atmospheric Environment, 34,* 3723-3733.

Kim, J.J., Smorodinsky, S., Lipsett, M., Singer, B.C., Hodgson, A.T., and Ostro, B. (2004). Traffic-related air pollution near busy roads: the East Bay children's respiratory study. *American Journal of Respiratory and Critical Care Medicine, 170 (5),* 520-526.

Kingham, S., Pearce, J., and Zawar-Reza, P. (2007). Driven to injustice? Environmental justice and vehicle pollution in Christchurch, New Zealand. *Transportation Research Part D, 12*, 254-263.

Kioutsioukis, I., Tarantola, S., Saltelli, A., and Gatelli, D. (2004). Uncertainty and global sensitivity analysis of road transport emission estimates. *Atmospheric Environment, 38,* 6609-6620.

Ko, J., Park, D., Lim, H., and Hwang, I. (2011). Who produces the most CO_2 emissions for trips in the Seoul metropolis area? *Transportation Research Part D, 16*, 358-364.

Kramer, U., Koch, T., Ranft, U., Ring, J., and Behrendt, H. (2000). Traffic-related air pollution is associated with atopy in children living in urban areas. *Epidemiology, 11 (1),* 64-70.

Kunzli, N., Kaiser, R., Medina, S., Studnicka, M., Chanel, O., Filliger, P., et al. (2000). Public-health impact of outdoor and traffic-related air pollution: a European assessment. *The Lancet, 356 (9232),* 795-801.

Langlois, A., and Kitchen, P. (1996). Identifying and measuring dimensions of urban deprivation in Montreal: An analysis of the 1996 census data. *Urban Studies, 50 (6),* 119-139.

Lindley, S.J., Conlan, D.E., Raper, D.W., and Watson, A.F.R. (1999). Estimation of spatially resolved road transport emissions for air quality management applications in North West region in England. *Science of the Total Environment, 235,* 119-132.

Logé, H. (2006). *2002-2003 Inventory of Greenhouse Gas Emissions*. Montréal Community, Ville de Montréal: Service des infrastructures, transport et environnement, Direction de l'environnement et du développement durable, Planification et suivi environnemental.

Lumbreras, J., Borge, R., Guijarro, A., Lopez, J.M., and Rodriguez, M.E. (2013). A methodology to compute emission projections from road transport (EmiTRANS). In press, *Technological Forecasting & Social Change.*

Mensink, C., de Vlieger, I., and Nys, J. (2000). An urban transport emission model for the Antwerp area. *Atmospheric Environment, 34,* 4595-4602.

Mitchell, G., and Dorling, D. (2003). An environmental justice analysis of British air quality. *Environment and Planning A, 35,* 909-929.

Nair, H.S., Bhat, C.R., and Kelly, R.J. (2000). Modeling soak-time distribution of trips for mobile source emissions forecasting: techniques and applications. *Transportation Research Record, 1750,* 24-31.

Nejadkoorki, F., Nicholson, K., Lake, I., and Davies, T. (2008). An approach for modelling CO_2 emissions from road traffic in urban areas. *Science of the Total Environment, 406,* 269-278.

NHTS. (2009). National Household Travel Survey 2009. "Number of Vehicle Miles (VMT) by Household Vehicle Count" Table, http://nhts.ornl.gov/tables09/FatCat.aspx?action=excel&id=28 accessed on March 20th 2013.

Padro-Martinez, L.T., Patton, A.P., Trull, J.B., Zamore, W., Brugge, D., and Durant, J.L. (2012). Mobile monitoring of particle number concentrations and other traffic-related air pollutants in a near-highway neighborhood over the course of a year. *Atmospheric Environment, 61,* 253-264.

Pampalon, R. and Raymond, G. (2000). A deprivation index for health and welfare planning in Quebec. *Chronic Diseases in Canada: A Publication of Health Canada, 21 (3),* 104-113.

PTV Vision. (2009). *VISUM 11.0 Basics.* Karlsruhe, Germany: PTV AG.

Sanchez-Cantalejo, C., Ocana-Riola, R., and Fernandez-Ajuria, A. (2008). Deprivation index for small areas in Spain. *Social Indicators Research, 89 (2),* 259-273.

Selander, J., Nilsson, M.E., Bluhm, G., Rosenlund, M., Lindqvist, M., Nise, G., and Pershagen, G. (2009). Long-term exposure to road traffic noise and myocardial infarction. *Epidemiology, 20 (2),* 272-279.

Shearmur, R., and Coffey, W.J. (2002). A tale of four cities: intrametropolitan employment distribution in Toronto, Montreal, Vancouver, and Ottawa-Hull, 1981-1996. *Environment and Planning A, 34,* 575-598.

Shearmur, R., and Motte, B. (2009). Weak ties that bind: do commutes bind Montreal's central and suburban economies? *Urban Affairs Review, 44 (4),* 490-524.

Smit, R., (2006). An examination of congestion in road traffic emission models and their application to urban road networks, PhD dissertation, Griffith University, Brisbane, Australia.

Smit, R., Ntziachristos, L, and Boulter, P. (2010). Validation of road vehicle and traffic emission models – a review and meta-analysis. *Atmospheric Environment, 44,* 2943-2953.

Societe de l'Assurance Automobile du Quebec (SAAQ) (2011). Vehicle Fleet Registry Data for the entire Province of Quebec.

Solis, J.C., and Sheinbaum, C. (2013). Energy consumption and greenhouse gas emission trends in Mexican road transport. *Energy for Sustainable Development, 17,* 280-287.

Statistics Canada. (2006). *2006 Census of Population*. Ottawa: Statistics Canada.

Statistics Canada. (2011). *2011 Census of Population.* Ottawa: Statistics Canada.

Statistics Canada. (2012). Greenhouse Gas Emissions from Private Vehicles in Canada, 1990 to 2007. "Households' greenhouse gas emissions from private vehicle operation, by census metropolitan area, 2007" Table, http://www.statcan.gc.ca/pub/16-001-m/2010012/t006-eng.htm accessed on August 8th 2013.

United States Environmental Protection Agency (USEPA). (1998). USEPA Assessment and Modeling Division Report on 'Modeling Hourly Diurnal Emissions and Interrupted Diurnal Emissions based on Real-Time Data'.

United States Environmental Protection Agency (USEPA). (2010). MOVES2010 highway vehicle: population and activity data. EPA-420-R-10-026, Assessment and Standards Division Office of Transportation and Air Quality U.S. Environmental Protection Agency.

Unger, N., Bond, T.C., Wang, J.S., Koch, D.M., Menon, S., Shindell, D.T., and Bauer, S. (2010). Attribution of climate forcing to economic sectors. *Proceedings of the National Academy of Sciences (PNAS), 107 (8)*, 3382-3387.

Waked, A., and Afif, C. (2012). Emissions of air pollutants from road transport in Lebanon and other countries in the Middle East region. *Atmospheric Environment, 61,* 446-452.

Wheeler, A.J., Smith-Doiron, M., Xu, X., Gilbert, N.L., & Brook, J.R. (2008). Intra-urban variability of air pollution in Windsor, Ontario – measurement and modelling for human exposure assessment. *Environmental Research, 106*, 7–16.

Woodcock, J., Banister, D., Edwards, P., Prentice, A.M., and Roberts, I. (2007). Energy and transport. *The Lancet, 370,* 1078-1088.

Xia, L., and Shao, Y. (2005). Modelling of traffic flow and air pollution emission with application to Hong Kong Island. *Environmental Modelling and Software, 20,* 1175-1188.

Zmirou, D., Gauvin, S., Pin, I., Momas, I., Sahraoui, F., Just, J. et al. (2004). Traffic related air pollution and incidence of childhood asthma: results of the Vesta case-control study. *Journal of Epidemiology & Community Health, 58,* 18-23.